HomOpt: A Flexible Homotopy-Based Hyperparameter Optimization Method

Sophia J. Abraham SABRAHA2@ND.EDU
Department of Computer Science and Engineering
University of Notre Dame
Notre Dame, IN 46556

Kehelwala D. G. Maduranga GMADURANGA@TNTECH.EDU
Department of Mathematics
Tennessee Tech University
Cookeville, TN 38505

Jeffery Kinnison JKINNISO@ND.EDU
Department of Computer Science and Engineering
University of Notre Dame
Notre Dame, IN 46556

Zachariah Carmichael ZCARMICH@ND.EDU
Department of Computer Science and Engineering
University of Notre Dame
Notre Dame, IN 46556

Jonathan D. Hauenstein HAUENSTEIN@ND.EDU
Department of Applied and Computational Mathematics and Statistics
University of Notre Dame
Notre Dame, IN 46556

Walter J. Scheirer WALTER.SCHEIRER@ND.EDU
Department of Computer Science and Engineering
University of Notre Dame
Notre Dame, IN 46556

Editor: TBD

Abstract

Over the past few decades, machine learning has made remarkable strides, owed largely to algorithmic advancements and the abundance of high-quality, large-scale datasets. However, an equally crucial aspect in achieving optimal model performance is the fine-tuning of hyperparameters. Despite its significance, hyperparameter optimization (HPO) remains challenging due to several factors. Many existing HPO techniques rely on simplistic search methods or assume smooth and continuous loss functions, which may not always hold true. Traditional methods like grid search and Bayesian optimization often struggle to adapt swiftly and efficiently navigate the loss landscape. Moreover, the search space for HPO is frequently high-dimensional and non-convex, posing challenges in efficiently finding a global minimum. Additionally, optimal hyperparameters can vary significantly based on the dataset or task at hand, further complicating the optimization process. To address these challenges, this paper presents `HomOpt`, an advanced HPO methodology that integrates a surrogate model framework with homotopy optimization techniques. Unlike rigid methodologies, `HomOpt` offers flexibility by incorporating diverse surrogate models tailored to specific optimiza-

tion tasks. Our initial investigation focuses on leveraging Generalized Additive Model (GAM) surrogates within the HomOpt framework to enhance the effectiveness of existing optimization methodologies. HomOpt's ability to expedite convergence towards optimal solutions across varied domain spaces, encompassing continuous, discrete, and categorical domains is highlighted. We conduct a comparative analysis of HomOpt applied to multiple optimization techniques (e.g., Random Search, TPE, Bayes, and SMAC), demonstrating improved objective performance on numerous standardized machine learning benchmarks and challenging open-set recognition tasks. We also integrate CatBoost within the HomOpt framework as a surrogate, showcasing its adaptability and effectiveness in handling more complex datasets. This integration facilitates an evaluation against state-of-the-art methods such as BOHB, particularly on challenging computer vision datasets like CIFAR-10 and ImageNet. Comparative analyses reveal HomOpt's competitive performance with reduced iterations and underscore potential optimizations in execution time. All the experimentation and method code can be found here: https://github.com/sabraha2/HOMOPT

1. Introduction

Selecting appropriate hyperparameters for a particular machine learning task is a challenging problem because of the vast search space, non-linear or non-monotonic effects on performance, and the complexity of the optimization landscape. Machine learning models consist of two distinct types of parameters: *elementary parameters*, which are learned during model training, and *hyperparameters*, which are higher-level free parameters that structure and control the training process. Most commonly, hyperparameters are set heuristically by practitioners before training, making the process prone to inconsistencies and biases across different individuals or experiments.

Automated machine learning (AutoML) aims to automate the entire machine learning pipeline, with automatic hyperparameter optimization (HPO) as a key subfield. HPO seeks to find the optimal hyperparameters for a given model to achieve the best possible performance on a specific task while improving reproducibility and fairness. By automating the HPO process, the search for optimal hyperparameters becomes more systematic and standardized, ensuring more consistent results when the same optimization algorithm is applied to the same problem. The performance of a model depends on the algorithm's architecture, the training data, and the chosen hyperparameters. Consequently, model selection is not solely an algorithmic determination, as hyperparameters significantly impact an algorithm's capability to learn. Hyperparameters, which can be real-valued, integer-valued, binary, or categorical, need to be set before training and differ from elementary parameters learned from the data. Hyperparameter search spaces serve as proxy domains for loss functions, which can be defined over nonlinear, non-convex spaces with many oscillations. This complexity makes the optimization process non-trivial. Identifying the best model for a particular learning task involves selecting hyperparameters to achieve the best performance on a specified task. This process is known as the hyperparameter optimization problem.

Various kinds of automated hyperparameter search approaches have been proposed to solve this optimization problem, ranging from simple methods like grid search (Duan and Keerthi, 2005) and random search (Bergstra and Bengio, 2012a), to more rigorous methods like Bayesian optimization (Bergstra et al., 2011a, 2015), gradient-based learning (Bengio, 2000; Maclaurin et al., 2015), and surrogate model approaches (Zhang et al., 2015). These methods have been used in many fields and have their own strengths and drawbacks. For example, grid search and random search are relatively simple to implement but can be computationally expensive and inefficient in exploring the hyperparameter space. Bayesian optimization is more efficient in searching the space but can

be sensitive to the choice of acquisition function and prior distributions. Gradient-based learning requires differentiable hyperparameters, which may not always be available, and surrogate model approaches depend on the quality of the surrogate model to guide the search effectively.

Our main contribution in this paper is the development of `HomOpt`, a flexible Hyperparameter Optimization (HPO) framework that employs homotopy optimization techniques alongside a variety of surrogate models (Figure 1), including Generalized Additive Models (GAMs) (Hastie and Tibshirani, 1990) and CatBoost (Prokhorenkova et al., 2018). `HomOpt` dynamically adapts to the complexities of the optimization task, effectively navigating the hyperparameter space to pinpoint optimal configurations. Utilizing a data-driven strategy, it sequences through a range of surrogate models that progressively refine our understanding of the hyperparameter landscape. This iterative process is designed to mitigate the "curse of dimensionality" often encountered in high-dimensional spaces (Nisbet, 2018, Chap. 7). Importantly, `HomOpt` implements a method where surrogates are continuously deformed to each other through homotopy, a concept foundational to our approach and previously exploited in other optimization contexts such as Iwakiri et al. (2022); Suzumura et al. (2017); Bates et al. (2013); Griffin and Hauenstein (2015); Chen and Hao (2019).

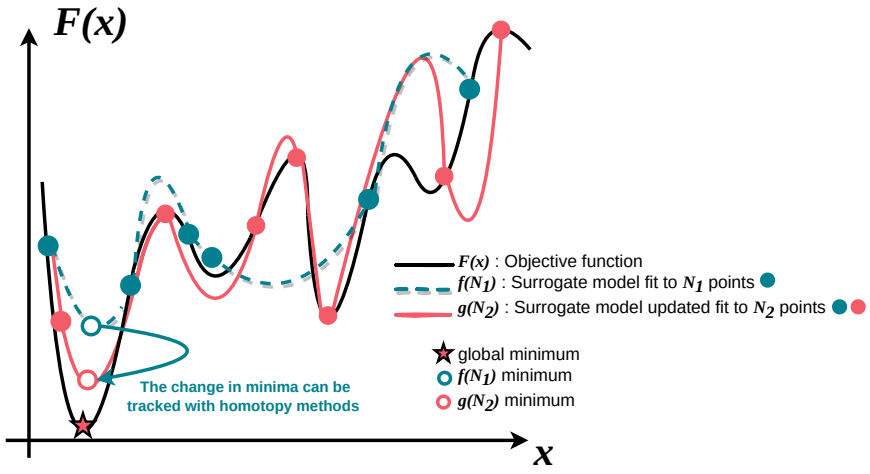

Figure 1: Illustration of homotopy parametrization between the initial samples and updated data samples. The black line represents the objective function that is being evaluated. The first surrogate model $f(N_1)$ is fit on the initial set of samples indicated by the blue circles. With more samples (indicated in pink), the updated surrogate $g(N_2)$ yields a new minimum. As the number of data samples increases, the approximation of the minimum improves. These changing minima can be tracked with homotopy methods.

`HomOpt` takes a new approach in hyperparameter optimization by integrating homotopy techniques with a versatile selection of surrogate models, enhancing adaptability and computational efficiency. Unlike traditional HPO methods that rely on static models, `HomOpt` utilizes the strengths of models like GAMs and CatBoost, adapting its strategy based on the evolving requirements of the task. This method improves search thoroughness in complex, high-dimensional spaces and reduces computational overhead by minimizing the number of model evaluations needed. Prior work by Iwakiri et al. (2022) and Suzumura et al. (2017) underscores the foundational use of homotopy in optimization, which `HomOpt` leverages to optimize performance trajectories.

One key aspect is that `HomOpt` can be used augment base optimization strategies. This flexibility is crucial in our experiments, where `HomOpt` is paired with traditional methods, such as

Random Search or Bayesian Optimization, to expedite the convergence process. By overlaying HomOpt on these base methods, we harness the strengths of both approaches, achieving faster convergence without sacrificing the thoroughness of the search. This is demonstrated in this paper in two distinct learning scenarios: closed-set and open-set learning. While closed-set learning only works on identifying predefined classes, open-set learning (Scheirer et al., 2012) trains models that have incomplete knowledge of the world they must operate in and allow the incremental learning setting, where newly identified classes are added to the recognition model over time. We conducted extensive experiments to showcase the efficacy of HomOpt in both closed-set and open-set learning scenarios with the Extreme Value Machine (EVM) (Rudd et al., 2017), which is a scalable nonlinear open-set classifier. The empirical analysis includes comparisons with state-of-the-art methods and sensitivity analyses on the meta-parameters of HomOpt, providing insights into its performance across diverse datasets and learning tasks.

Additionally we introduce CatBoost into the HomOpt framework as a surrogate, targeting complex, high-dimensional datasets such as CIFAR-10 and ImageNet. CatBoost, a gradient boosting algorithm that excels in handling categorical features and complex data structures, is employed to navigate the hyperparameter spaces of deep learning models effectively. This integration showcases HomOpt's adaptability, achieving notable reductions in the number of optimization iterations and demonstrating the potential to enhance execution times, thereby showing a competitive edge over existing state-of-the-art methods.

To summarize, our contributions are the following:

1. **Adaptability and Efficiency:** HomOpt achieves improvement in optimization efficiency and adaptability across various problem domains by intelligently approximating local regions of interest within the hyperparameter space, rather than attempting to model the entire surface. This approach, grounded in the principles of homotopy and the Morse lemma, enables HomOpt to adaptively navigate complex landscapes and converge to optimal solutions more rapidly than traditional methods.

2. **Applicability to Diverse Domains:** HomOpt can be applied across a spectrum of search domains, including continuous, discrete, and categorical spaces. This wide applicability is facilitated by HomOpt's model-agnostic framework, which can incorporate various types of surrogate models to align with the specific characteristics of the optimization problem. This adaptability attests to HomOpt's flexibility, enabling effective optimization in diverse settings and showcasing its utility beyond the confines of traditional hyperparameter optimization.

3. **Theoretical and Empirical Advantages over Existing Homotopy Methods:** Our work not only introduces a novel integration of homotopy optimization with surrogate modeling but also establishes theoretical and empirical advantages over prior homotopy optimization efforts. By leveraging the dynamic sequencing of surrogate models and employing a new continuous deformation approach, HomOpt achieves more stable and efficient optimization trajectories. This methodology is validated through extensive experimentation, demonstrating HomOpt's ability to outperform traditional optimization methods in a variety of machine learning contexts.

4. **Universal Compatibility with Loss Functions:** HomOpt is designed to be universally compatible with any type of loss function, making it a highly versatile tool for a broad array of

optimization problems. This universality is crucial for its application across different machine learning tasks and models, ensuring that `HomOpt` remains effective regardless of the specific nature or complexity of the objective function.

5. **Open-Source Contribution:** In addition to the theoretical and practical advancements introduced by `HomOpt`, we contribute to the community by releasing a flexible, and open-source software package. This package facilitates the application of `HomOpt` to a wide range of search problems, enabling researchers and practitioners to rapidly deploy `HomOpt` in their optimization tasks. All code and data is available at `https://github.com/sabraha2/HOMOPT`.

2. Related Work

Basic Hyperparameter Optimization. Hyperparameter optimization methods involve searching for optimal hyperparameter values to effectively identify high-performing models within the hyperparameter space. Non-Bayesian approaches, such as hand-tuning and grid search (Duan and Keerthi, 2005), are simple to use. However, they rely upon adequate domain knowledge, which may not readily be available. Furthermore, these methods may overlook optimal values in continuous domains and inevitably prove brittle when applied to unseen cases (Li et al., 2017). Random search (Bergstra and Bengio, 2012a) mitigates this issue by removing the requirement of discretizing the search space and provides a larger coverage of the hyperparameter space. Although random search is simple to use, it is often inefficient sampling-wise. In order to narrow the scope of the search, multiple software frameworks for hyperparameter search based on random search have been proposed, including those by Bergstra et al. (2015, 2011a); Betrò (1992); Wu et al. (2019); Bengio (2000); Maclaurin et al. (2015); Ilievski et al. (2017).

Population-Based Approaches. Population-based algorithms take inspiration from biology and improve upon computational efficiency over purely random search-based methods (Loshchilov and Hutter, 2016). These methods include Evolutionary Algorithms and swarm algorithms like particle swarm optimization (PSO) (Boeringer and Werner, 2005), which iteratively update the generation of hyperparameters with a stochastic velocity term. While effective for lower dimensional spaces, methods like PSO can get stuck in a local optimum for high dimensional, complex scenarios with low convergence rates over the iterative process (Kennedy and Eberhart, 1995).

Bayesian Optimization. In order to perform the search using statistical analysis, Bayesian optimization methods have been proposed (Bergstra et al., 2015, 2011a; Betrò, 1992; Wu et al., 2019) based on Bayes' theorem. It sets a prior over the optimization function and gathers the information from the previous sample to update the posterior of the optimization function. A utility function selects the next sample point to maximize or minimize the optimization function. One example of a popular Bayesian method is the Sequential Model-Based Algorithm Configuration (SMAC) (Lindauer et al., 2017) consisting of Bayesian optimization combined with a simple racing mechanism on the instances to efficiently decide which of two configurations performs better.

Tree-Structured Parzen Estimators (TPE) (Bergstra et al., 2011a, 2015), which is another Bayesian method, is a sequential model-based optimization (SMBO) approach. SMBO methods sequentially construct models to approximate the performance of hyperparameters based on historical measurements, and then subsequently choose new hyperparameters to test with based on a constructed model.

Gradient-based Approaches. Gradient-based optimization methods (Bengio, 2000; Maclaurin et al., 2015) compute gradients of cross-validation performance with respect to all hyperparameters by chaining derivatives backwards through the entire training procedure. This is advantageous over other methods since information regarding the shape of the objective surface and behaviors including extrema in the parameter space can be acquired. Hyperparameter gradients are computed by reversing the dynamics of stochastic gradient descent. Gradients enable the optimization of the hyperparameters, including step-size, momentum schedules, weight initialization distributions, richly parameterized regularization schemes, and neural network architectures. However, information about the gradients is often unavailable, computing gradients is computationally expensive, and gradient-based approaches suffer from inefficiency when learning long-term dependencies (Bengio et al., 1994).

Surrogate-based Approaches. Surrogate-based optimization methods (Eggensperger et al., 2014; Xie et al., 2021; McLeod et al., 2018) are used when an objective function is expensive to evaluate. The Surrogate Benchmarks for Hyperparameter Optimization (Eggensperger et al., 2014) uses the following strategy: cheap-to-evaluate surrogates of real hyperparameter optimization benchmarks that yield the same hyperparameter spaces and feature-similar response surfaces. Specifically, this approach trains regression models on data representing a machine learning algorithm's performance under a broad range of hyperparameter configurations and then cheaply evaluates hyperparameter optimization methods using the model's performance predictions instead of the actual algorithm. In McLeod et al. (2018), a Gaussian Process-based (GP) model was used to identify a convex region and a probability-based approach was used to estimate a convex region centered around the posterior minimum. Our approach uses the exploitation from multiple optimization techniques to identify the region of interest for surrogate approximation.

Homotopy-based Approaches. Homotopy methods, also known as continuation methods, have established their value across numerous fields of numerical analysis, providing solutions to diverse mathematical and engineering challenges. These methods work by iteratively transitioning from straightforward to complex problem settings, a process that facilitates globally convergent and comprehensive solutions for nonlinear problems (Rheinboldt, 1981; Allgower and Georg, 1990; Bates et al., 2013). While traditionally leveraged in areas outside of HPO, homotopy methods are beginning to show promise within this domain, offering potential advantages in training efficiency and model accuracy that have yet to be fully explored in comparison to conventional optimization techniques. Early applications to machine learning by Chow et al. (1991), followed by Pathak (2018); Chen and Hao (2019); Mehta et al. (2022), have utilized data continuation and model continuation strategies. These approaches aim to simplify the original optimization task into a series of incrementally challenging stages, primarily focusing on elementary parameter optimization and model initialization.

Extending beyond these foundational applications, recent studies by Iwakiri et al. (2022) and Suzumura et al. (2017) have applied homotopy methods to hyperparameter tuning for specific machine learning models, such as support vector machines and neural networks. These efforts underscore the efficiency and effectiveness of homotopy methods in navigating the intricate hyperparameter spaces, yielding improvements over traditional techniques like grid search. Building upon these advancements, our contribution with the `HomOpt` framework broadens the scope of homotopy methods to a more generalized application in HPO across an extensive range of machine learning algorithms. `HomOpt` distinguishes itself by incorporating a dynamic selection of surrogate models, including GAMs for their interpretability and CatBoost for managing complex datasets. This ap-

proach not only adheres to the foundational principles of homotopy but also significantly enhances its adaptability and utility for contemporary machine learning challenges.

Moreover, `HomOpt` aligns with insights from Mehta et al. (2022) on the application of homotopy for understanding neural network loss surface topology. Although Mehta et al. do not directly address HPO in their work, they provide valuable perspectives on leveraging homotopy methods to overcome optimization obstacles. These insights are integral to the objectives of the `HomOpt` framework. Our work moves beyond the initial limited scope of homotopy applications in machine learning, proposing a flexible and comprehensive approach to HPO that aims to improve the efficiency and efficacy of model tuning across a diverse array of machine learning algorithms and datasets.

The prior work on hyperparameter optimization leveraging homotopy methods presents compelling advancements that `HomOpt` seeks to build upon. The work by Felten et al. (2023) develops a two-phase hyperparameter optimization approach for multi-objective reinforcement learning, integrating homotopy optimization to systematically adjust hyperparameters from simple to complex configurations. This method not only highlights its versatility but also demonstrates its potential to streamline the optimization process in complex multi-objective environments. Similarly, Liu et al. (2023) harness homotopy within a Bayesian Optimization framework to address the challenges of HPO, providing a novel perspective on integrating these methods for more efficient model tuning.

While continuation algorithms as discussed in Rojas-Delgado et al. (2022) provide a direct approach to hyperparameter optimization by transforming a surrogate of the fitness function progressively to approximate the true fitness function, `HomOpt` takes a different approach by embedding these algorithms within a homotopy framework. Unlike the approach where continuation primarily simplifies the fitness landscape statically, `HomOpt` employs a dynamic homotopy process that not only transitions between different surrogate models but also adapts these models in response to new data. This dynamic adaptation allows `HomOpt` to efficiently navigate complex hyperparameter landscapes by exploiting the structured continuity of homotopy, which methodically explores the path of least resistance between local optima across evolving surrogate models.

This use of homotopy extends the traditional application of continuation algorithms by incorporating a sequence of surrogate models that are continuously updated. Each model in the sequence is designed to capture increasingly accurate representations of the underlying hyperparameter space, thus facilitating a more granular optimization process compared to fixed-model methods like Differential Evolution (Storn and Price, 1997). In essence, `HomOpt` not only follows the continuity principle inherent in continuation methods but also enhances it through strategic model transitions, which are governed by both the homotopy paths and the insights gained from new data accumulations. This approach allows for a flexible, yet precise, exploration and exploitation strategy that is robust to the typical pitfalls of high-dimensional optimization, such as the curse of dimensionality and local optima entrapment.

3. Homotopy-Based Hyperparameter Optimization

We propose a new data-driven hyperparameter optimization approach that efficiently navigates the complex landscape of model parameters through the integration of surrogate modeling and homotopy techniques. The efficacy of the `HomOpt` framework (Algorithm 1) in navigating the hyperparameter optimization landscape hinges on the selection of surrogate models and the construction of an appropriate homotopy between them. First, surrogates are used to model the objective since

Algorithm 1: Homotopy Optimization Framework

Input: Timeframe $\mathcal{T}$, trial limit $\mathcal{N}_{\mathcal{T}}$, sample size $\mathcal{W}$, localization threshold $\mathcal{D}$, sampling method `Inner_Method`, data fraction k.
Output: Optimal hyperparameter set.
Initialize: Counter $\mathcal{C}_{\mathcal{T}} \leftarrow 0$, trial data.
while *within time $\mathcal{T}$ and trial limit $\mathcal{N}_{\mathcal{T}}$* **do**
    if *preliminary phase or at specific intervals* **then**
        Sample hyperparameters via `Inner_Method`.
    else if *designated intervals* **then**
        Adjust parameters by perturbation, focusing on the best within $\mathcal{D}$.
    else
        // Train exploration model f on a selected fraction of recent data.
        // Train exploitation model g on top-performing configurations or updated dataset
        Employ homotopy optimization (see Alg. 2), transitioning from exploration to exploitation models, to identify promising candidates.
        Evaluate new candidates, refresh trial data.
    end
    Update trial data with new evaluations.
end
Derive the set with minimum loss from trial data as the optimal set.

Algorithm 2: Homotopy Optimization

Input $\mathcal{N}$ number of steps along interval, homotopy function $H(x,t)$, $x^{(0)} = x^0$ a local minimum of $H(x,1)$
Output Local minimum of $H(x,0)$
$\Delta \leftarrow 1/\mathcal{N}$
$t \leftarrow 1$
for $k \leftarrow 1$ *to* $\mathcal{N}$ **do**
    $t \leftarrow t - \Delta$
    Use Nelder-Mead optimization to minimize $H(x,t)$ starting with $x^{(k-1)}$ to obtain $x^{(k)}$.
return $x^{(N)}$

the function and its gradient are computationally expensive to evaluate. In particular, a sequence of surrogate models is constructed as new data is gathered. A continuous deformation from the current surrogate model to the updated one that includes the new data is formed. Second, leveraging the concept of continuous deformation further, `HomOpt` utilizes homotopy to establish a pathway between local optima of consecutive surrogate models. This methodical approach not only enhances the efficiency of the optimization process but is also underpinned by solid mathematical foundations, promoting a more consistent convergence towards optimal parameters with reduced iterations. `HomOpt`'s design is deliberately model-agnostic, offering the flexibility to incorporate various types of surrogate models to suit different optimization challenges.

The first step is to select a family of surrogate models. The versatility in surrogate model selection positions `HomOpt` to adaptively align with the problem's characteristics more effectively than fixed-model methods like Differential Evolution (Storn and Price, 1997), particularly in complex or high-dimensional spaces where the objective function's nature challenges traditional assumptions. This adaptability is a critical advantage in environments with non-convex, noisy, or discontinuous loss functions, though it necessitates judicious surrogate model selection to mitigate misalignment risks with the optimization landscape (Forrester et al., 2008). Some examples include polynomial spline fitting with several degrees of freedom and radial basis function interpolation. Selecting an appropriate surrogate model involves evaluating the model's capacity to approximate the true loss function's behavior across the hyperparameter space. Mathematically, this capacity can be characterized by the model's *approximation error*, ϵ, defined as the difference between the true loss function, $L(\boldsymbol{x})$, and the surrogate model's prediction, $M(\boldsymbol{x})$, over the hyperparameter vector $\boldsymbol{x}$ (Forrester and Keane, 2009; Tibshirani and Hastie, 1987):

$$\epsilon(\boldsymbol{x}) = |L(\boldsymbol{x}) - M(\boldsymbol{x})|. \tag{1}$$

The choice between models hinges on minimizing this error across the domain of interest. In our investigation, we demonstrate the adaptability and breadth of `HomOpt` through the deployment of two distinct surrogate models. We use a generalized additive model (GAM) (Hastie and Tibshirani, 1990), which is a type of statistical model that is used to describe the relationship between a response variable and one or more predictor variables and Catboost, a gradient boosting library that is specifically designed to handle categorical features. GAMs, with their flexibility to model nonlinearities through smooth functions, are particularly suited for datasets where the relationship between hyperparameters and the loss function is expected to be smooth but complex. This is supported by the model's ability to fit additive smooth functions, $s_i(x_i)$, for each hyperparameter x_i, optimizing the smoothness penalty to prevent overfitting (Hastie and Tibshirani, 1990). GAMs are similar to generalized linear models (GLMs), but they allow for nonlinear relationships between the response (output or target variable we try to predict) and predictor variables (input features used to make the prediction) by using smooth functions to model the relationships. These can be estimated using penalized regression techniques, such as penalized splines, and they can provide more flexible and accurate models than GLMs in many cases. The results of some initial empirical experiments along with some theoretical advantages described below suggest that the extrapolation behavior is more reasonable for GAMs and, for multidimensional data, is more suitable and provides a more accurate fit. In our implementation we utilize GAMs via PyGAM (Servén et al., 2018).

From a theoretical standpoint, GAMs provide a more interpretable model than other surrogate models as the smoothing functions that are used to model the relationships between the response and predictor variables can be visualized and analyzed directly. This can be especially useful for understanding and explaining the underlying patterns and relationships in the data, which can be difficult to do with more complex and opaque models like random forests. Additionally, GAMs can provide more accurate predictions for certain types of data, such as data with nonlinear or non-monotonic relationships between the response and predictor variables. Moreover, relationships between the response and predictor variables in GAMs can provide insight into the importance of each feature. For example, the magnitude and significance of the coefficients of the smoothing functions can be used to determine the relative importance of each feature, and the shape of the smoothing function can provide additional information about the nature of the relationship between the response and predictor variables. Although a detailed theoretical analysis of these aspects is

beyond the scope of this paper, they represent a powerful tool for understanding and interpreting the results of the hyperparameter optimization process. For practical demonstration, additional visualizations and analyses that illustrate these capabilities in optimizing the Branin function are presented in Appendix B.

In contrast, models like CatBoost are ensemble methods that offer robust performance in the presence of categorical variables and complex interaction effects. Their suitability can be assessed through the *ensemble diversity*, δ, which measures the variance in predictions across the ensemble, providing an indication of the model's ability to explore the parameter space (Liaw et al., 2002; Dorogush et al., 2017; Prokhorenkova et al., 2018):

$$\delta = \mathrm{Var}\left(\{M_i(\boldsymbol{x})\}_{i=1}^{N}\right), \tag{2}$$

where $M_i(\boldsymbol{x})$ denotes the prediction of the i-th model in the ensemble for hyperparameters $\boldsymbol{x}$, and N is the number of models in the ensemble. CatBoost stands out for its efficient handling of categorical features and robust gradient boosting mechanism, making it an invaluable tool for exploring and exploiting the hyperparameter space. Unlike traditional boosting algorithms, CatBoost does not require extensive preprocessing of categorical features, thereby streamlining the optimization process. Moreover, its gradient boosting mechanism enables iterative refinement of predictions, allowing `HomOpt` to dynamically balance exploration and exploitation strategies. This capability is crucial for efficiently navigating through the hyperparameter space and identifying promising regions for further exploration.

Following the selection of the family of surrogate models, the second step is to construct a continuous deformation between surrogate models as new data is collected and then utilize homotopy methods (Algorithm 2) to track a local minimum along this deformation as illustrated in Figure 2. Unlike discrete methods such as Bayesian Optimization with Gaussian Processes (Rasmussen et al., 2006) or Tree Parzen Estimator (Bergstra et al., 2011b), `HomOpt`'s continuous approach allows for a refined search near promising areas, potentially uncovering superior optima (Watson et al., 1997). The choice of homotopy plays a crucial role in navigating from one surrogate model to another. While linear homotopy offers simplicity and ease of implementation, alternative forms could potentially offer more nuanced transitions, accommodating regions of the hyperparameter space where the loss function's gradient undergoes significant changes. The decision to employ a linear versus a non-linear homotopy can be informed by examining the *transition smoothness*, σ, defined as:

$$\sigma = \int_0^1 \left\| \frac{dH}{dt} \right\| dt, \tag{3}$$

where $\left\| \frac{dH}{dt} \right\|$ measures the norm of the derivative of H with respect to t, quantifying the rate of change in the homotopy path, guiding the selection of a linear versus non-linear approach (Allgower and Georg, 1990; Yamamura et al., 1999). A smaller value of σ indicates a smoother transition, potentially leading to more stable optimization trajectories.

For a general overview of homotopy methods, with a focus on nonlinear polynomial functions, see (Bates et al., 2013). In the context of optimization using surrogate models that depend upon continuous variables, local minima are critical points of the surrogate model, *i.e.*, the gradient of the surrogate model vanishes at each local minimum. Although computing all critical points of the objective function using homotopy methods has shown to be useful in some applications (Mehta et al., 2022; Baskar et al., 2022), the approach utilized here does not rely upon computing all critical points

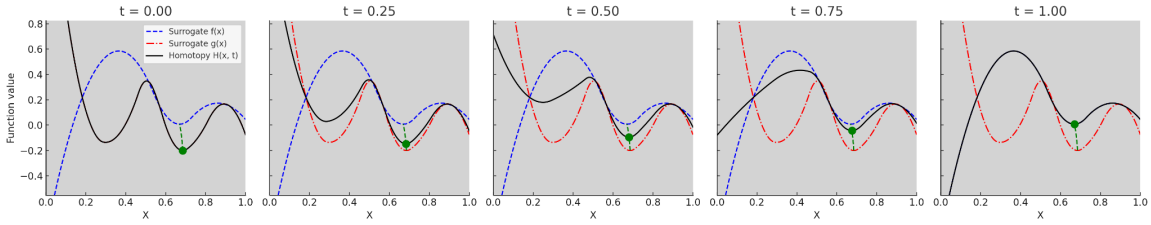

Figure 2: ***Evolution of Minima Using the Homotopy Method****: This figure illustrates the iterative refinement of minima through the application of the homotopy method in surrogate model optimization. The process begins with the construction of surrogate models, $f(x)$ and $g(x)$, based on initial and expanded data samples, respectively. The homotopy function $H(x, t)$ smoothly transitions between these surrogates as t varies from 0 to 1. The green circles represent the local minima of $H(x, t)$ at different t values, illustrating the dynamic nature of the optimization process. The path of these evolving minima is traced across the homotopy, highlighting the progress in approximating the optimal solution.*

to provide a scalable framework to higher-dimensional and non-polynomial systems. The versatility of `HomOpt` is demonstrated through two distinct implementations using Generalized Additive Models (GAM) and CatBoost models, each demonstrating the framework's dynamic adaptability to evolving datasets and optimization goals.

3.1 Implementation with Generalized Additive Models (GAM)

We begin with a GAM, represented as $f(x)$, tailored to an initial dataset of N_1 observations. This model acts as the surrogate for the objective function in an unconstrained optimization environment, where an initial local minimum, x_{old}, is pinpointed. Upon acquiring new observations, expanding the dataset to N_2 points, we transition to an updated GAM, $g(x)$. To make this transition, we deploy a linear homotopy to facilitate a seamless deformation from f to g. This establishes a dynamic pathway through the optimization landscapes of the surrogate models:

$$H(x,t) = t \cdot f(x) + (1-t) \cdot g(x), \quad \text{where} \quad H(x,1) = f(x), \quad \text{and} \quad H(x,0) = g(x). \tag{4}$$

This methodology introduces a family of unconstrained optimization problems, defined by the objective function $H(x, t)$, with a known local minimum at $t = 1$ transitioning from x_{old}. It thus delineates a homotopy path of local minima, parameterized by t, emanating from x_{old} towards a new local optimum, x_{new}, as t shifts to 0. Employing standard homotopy theory (Sommese and Wampler, 2005) when f and g are analytic offers guarantees on the path's existence and smoothness, culminating at the desired local minima x_{new} at $t = 0$. Our framework is designed to tackle a broad spectrum of HPO problems, employing strategies like Nelder-Mead optimization (Nelder and Mead, 1965), which do not depend on the smoothness or differentiability of the surrogate models.

3.2 Implementation with CatBoost Models

We extend our approach to incorporate CatBoost models, aiming to deepen our exploration of the homotopy concept within HPO. We introduce two CatBoost models, denoted as $f(x)$ for exploration and $g(x)$ for exploitation, each serving a specific strategic purpose.

Exploration Model $f(x)$: Tailored to probe the hyperparameter space, $f(x)$ is trained across a broad dataset of hyperparameter configurations and their associated performance outcomes to

identify unexplored, potentially high-performing regions. This model leverages the predictive power of CatBoost to forecast promising areas within the parameter space that merit further optimization.

Exploitation Model $g(x)$: This model concentrates on optimizing within regions previously recognized for their potential. It aims to intensify the search and optimization efforts in these selected areas, improving the precision and effectiveness of the HPO process.

The `HomOpt` framework employs a dynamic optimization approach, modulated by a homotopy parameter t, to balance between the exploration and exploitation models. The optimization trajectory is again governed by:

$$H(x,t) = t \cdot f(x) + (1-t) \cdot g(x),$$

where t is systematically adjusted to ensure a seamless transition from broad exploration to focused exploitation. This methodical strategy for generating new configurations and evaluating them against the combined output of $f(x)$ and $g(x)$ demonstrates the framework's capacity for adaptability. Moreover, it reflects how iterative refinement, informed by continuous feedback, enhances the HPO strategy.

3.3 One-Dimensional Illustration

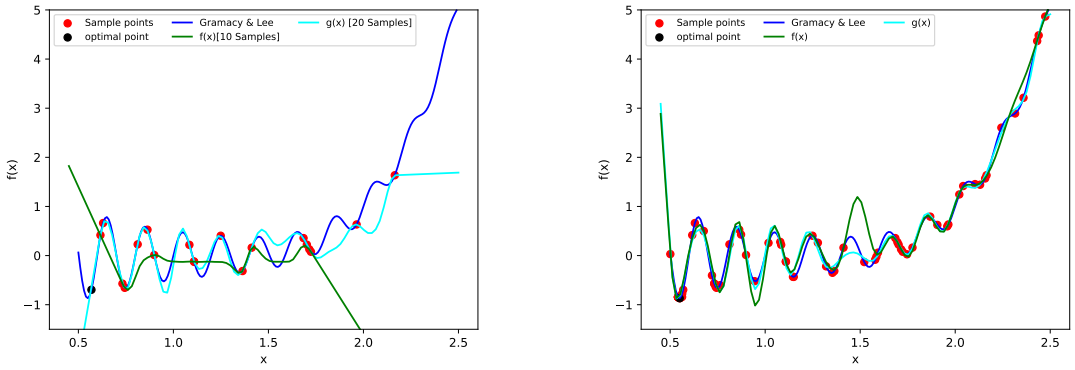

(a) Start of optimization

(b) After 8 optimization steps

Figure 3: The Plot of the Gramacy and Lee function on the domain $[0.5, 2.5]$ (blue curve). The strategy used by `HomOpt` is to find a homotopy continuation path from the minimum of $f(x)$ to the minimum of the $g(x)$. (a) Local surrogate approximations of $f(x)$ (green curve), and surrogate approximation of $g(x)$ (cyan curve) at the initial stages. (b) Local surrogate approximations of $f(x)$ (green curve), and surrogate approximation of $g(x)$ (cyan curve) after eight homotopy optimization steps.

To illustrate `HomOpt`, we consider the optimization of the test function $p(x)$ defined by (Gramacy and Lee, 2012) on the domain $[0.5, 2.5]$, where

$$p(x) = \frac{\sin(10\pi x)}{2x} + (x-1)^4. \tag{5}$$

The plot of $p(x)$ is shown in blue in Figure 3. Consider two GAMs f and g constructed from 10 and 20 sample points, respectively, as shown in Figure 3(a). Note that the number of samples used in

f and g were selected arbitrarily for illustration purposes. The strategy for `HomOpt` is to consider the homotopy path from a known local minimum of $f(x)$ to a local minimum of $g(x)$ that we want to compute. Figure 3(b) shows the optimized surrogate curves $f(x)$ and $g(x)$, along with the corresponding optimal point obtained after eight iterations of the `HomOpt` method demonstrating convergence to the global minimum.

3.4 Two-Dimensional Example

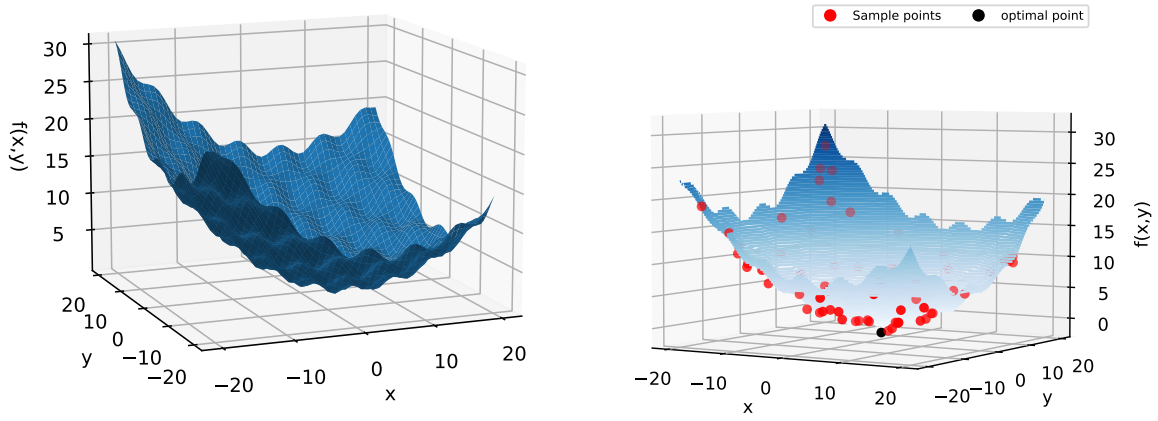

(a) Griewank Function *(b) `HomOpt` convergence to optimal point*

Figure 4: (a) Plot of the modified Griewank function on the domain $[-20, 20]^2$. (b) `HomOpt` converged towards the optimal point shown (black point) using 100 randomly sampled points (red points).

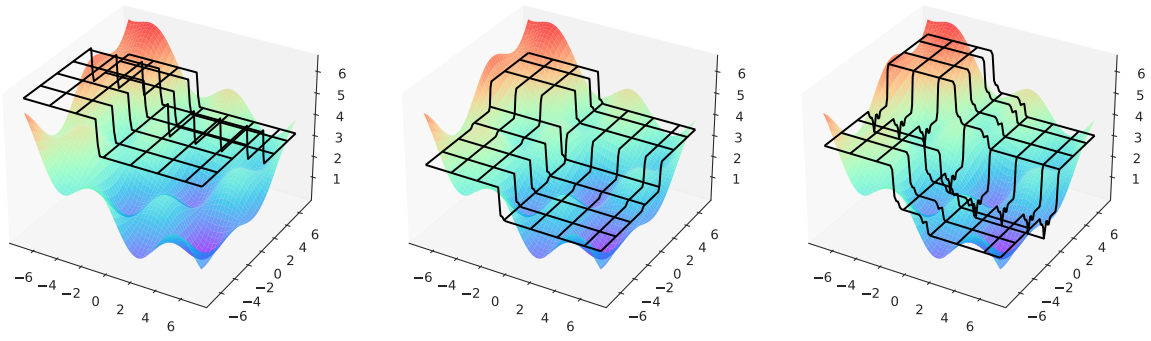

(a) Surrogate from 10 samples *(b) Surrogate from 20 samples* *(c) Surrogate from 40 samples*

Figure 5: Plots of the modified Griewank function on the domain $[-7, 7]^2$ with the surrogate approximation plotted as a black grid fit to different numbers of samples. As the numbers of samples increases, the surrogate function begins to get a better approximation of the underlying function and converge towards the global optimum.

Now consider the two-dimensional case. The Griewank function, introduced by Griewank (Surjanovic and Bingham, 2013), is a standard test example in optimization problems in the 2D plane. However, to prevent the global minimum from being located at the origin and increase the difficulty of the problem, a modified function is considered over the domain $[-20, 20]^2$:

$$g(x, y) = \frac{(x-5)^2 + (y+3)^2}{40} - \cos(x-5) \cdot \cos\left(\frac{y+3}{\sqrt{2}}\right) + 1 \tag{6}$$

which is plotted in Figure 4(a).

In Figure 4(b), the optimal point (in black) for the Griewank function is shown along with the sampled points (in red). `HomOpt` was able to successfully converge to the optimal point within 100 sampled points. The Griewank function is relatively simple and a low-dimensional problem and as such 100 sampled points was sufficient to accurately approximate the objective function and converge to the optimum. It is important to note that for more complex and higher dimensional problems, it may be necessary to use a larger number of sampled points. As depicted in Figure 5, the black grid representing the approximation of `HomOpt` improved as more sample points were added, learning the overall shape of the Griewank function within 40 sample points.

3.5 Optimization Software Framework Integration

Our work is designed to extend the Scalable Hardware-Aware Distributed Hyperparameter Optimization (SHADHO) framework, known for its versatility in executing a wide array of hyperparameter optimization strategies, including Random Search, Bayesian Optimization, Particle Swarm Optimization (PSO), Sequential Model-based Algorithm Configuration (SMAC), and Tree-structured Parzen Estimator (TPE) (Kinnison et al., 2018). SHADHO is designed for distributed computing environments, offering a scalable solution for complex machine learning model optimization across extensive hyperparameter spaces. A unique feature of SHADHO is its capability to incorporate hardware specifications into the optimization process, optimizing computational resources alongside model performance metrics.

Building upon SHADHO's software framework, we introduce the extension of the integration of `HomOpt`. This extension specifically takes advantage of GAM approach. This method dynamically adapts to the evolving data landscape, training surrogate models on fractions of the data determined by the parameter k, and iteratively refining the search for optimal hyperparameters via a homotopy process. Our method stands out by its employment of random perturbations and Nelder-Mead optimization, aimed at discovering and converging to local optima with enhanced precision.

In parallel, we've conducted experiments outside SHADHO's immediate framework using CatBoost to investigate `HomOpt` not only in the context of boosting base strategies but to also compare it directly against state of the art methods. Despite the robust capabilities of SHADHO in distributed hyperparameter optimization, it currently lacks specific integrations necessary for running the complete set of HPOBench benchmarks. We adopt a similar homotopy-inspired approach but pivots towards CatBoost's strengths in handling categorical features and complex data relationships. By alternating between exploration and exploitation models within the CatBoost framework, this optimizer fine-tunes the hyperparameter search, showcasing the flexibility and adaptability of the `HomOpt` method across different surrogate models. This specific implementation and all of the experimentation scripts is available for reproducibility[1].

1. See repository at `https://github.com/sabraha2/HOMOPT`

HomOpt's can seamlessly integrate with existing optimization frameworks like SHADHO, providing a powerful, scalable solution for hyperparameter tuning. The source code for SHADHO's latest release, featuring HomOpt, is available for the community to explore and further develop[2].

4. Experiments

We evaluate HomOpt on a multitude of tasks. We begin with a collection of machine learning benchmarks for classification tasks on tabular data using a Multi-Layer Perceptron (MLP), Support Vector Machine (SVM), Random Forest, XGBoost, and Logistic Regression provided through HPOBench (Eggensperger et al., 2021).

Additionally, we include a set of difficult *open-set* classification experiments. In the open-set scenario, models have incomplete knowledge of the world they must operate in and unknown classes are queried during testing (Scheirer et al., 2012). Open-set classification is notoriously sensitive to hyperparameters and provides a complex scenario where the loss landscape is arbitrary, polluted by noise, and may consist of steep gradients resulting in the absence of regularity. This set of experiments also captures how well HomOpt can boost methods in changing environments and unseen conditions.

We use the Extreme Value Machine (EVM) (Rudd et al., 2017), which is a scalable nonlinear classifier that supports open-set classification by rejecting inputs that are beyond the support of the training set. The EVM relies on a strong feature representation and every represented sample in the feature representation becomes a point. It utilizes a binning strategy that groups all the points in their feature representation by their corresponding label. These bins are utilized to create a "1 vs. rest" classifier for each known class. It generates a classifier where a Weibull distribution is fit on the data for each known class and is made to avoid the negative data points (unknown classes). This process is repeated for all known classes. When a new data point (a sample represented by its feature vector) is provided to the EVM, it is evaluated in the feature space, and the probability of the point belonging to each representative class is determined.

Parameter	**Description**	**Domain**
Threshold	Probability threshold used to determine if an input coordinate point should be classified as 'unknown' if the point falls below this probability of inclusion.	$[0, 1]$
Tailsize	Defines how many negative samples are used to estimate the model parameters.	$[0, 0.5]$
Cover threshold	The probability threshold used to eliminate extreme vectors if they are covered by other extreme vectors with that probability.	$[0, 1]$
Distance multiplier	The multiplier to compute margin distances.	$[0, 1]$
Distance function	The distance function used to compute the distance between two samples.	Cosine or Euclidean

Table 1: Hyperparameters used in training the EVM.

2. See the extended SHADHO framework at https://github.com/jeffkinnison/shadho

Table 2: OpenML Task IDs used for HPOBench experiments. The table displays the total number of instances (combining the training and testing sets) (#obs) and the number of features prior to any preprocessing (#feat) for each dataset.

Name	TID	#obs	#feat
blood-transf..	10101	748	4
vehicle	53	846	18
Australian	146818	690	14
car	146821	1728	6
phoneme	9952	5404	5
segment	146822	2310	19
credit-g	31	1000	20
kc1	3917	2109	22
sylvine	168912	5124	20
kr-vs-kp	3	3196	36
jungle_che..	167119	44819	6
mfeat-factors	12	2000	216
shuttle	146212	58000	9
jasmine	168911	2984	145
cnae-9	9981	1080	856
numerai28.6	167120	96320	21
bank-mark..	14965	45211	16
higgs	146606	98050	28
adult	7592	48842	14
nomao	9977	34465	118

The hyperparameters involved in training the EVM are included in Table 1. The datasets used in the HPOBench experiments can be found in Table 2 and the benchmark details along with their configuration spaces can be found in Table 3. For further specifications regarding specifics on the benchmarks and datasets from HPOBench please refer to the original paper (Eggensperger et al., 2021).

Furthermore, we assess the efficacy of `HomOpt` using CatBoost surrogate models on the challenging NB201 neural architecture search (NAS) tabular benchmarks (Dong and Yang, 2020) within HPOBench, targeting the CIFAR-10 and ImageNet16-12 0 datasets. This evaluation not only demonstrates `HomOpt`'s ability to improve base methods, but compares `HomOpt` directly against state-of-the-art black box and multi-fidelity optimization techniques, allowing us to measure its performance in a comparative landscape. In this context, fidelity refers to the accuracy and complexity of the model evaluations used to optimize the objective function. Lower-fidelity models typically offer quicker but less accurate evaluations, while high-fidelity models provide more accurate but computationally expensive evaluations. It is important to note that unlike multi-fidelity methods, which vary the accuracy and computational expense of model evaluations, `HomOpt` consistently applies a single-fidelity approach throughout the optimization process. This approach ensures uni-

Table 3: Configuration spaces for the benchmarks included in HPOBench, with hyperparameters and their ranges for each model.

Benchmark	Name	Range
SVM	C	$[2^{-10}, 2^{10}]$
	gamma	$[2^{-10}, 2^{10}]$
LogReg	alpha	[1e-05, 1.0]
	eta0	[1e-05, 1.0]
XGBoost	colsample_bytree	[0.1, 1.0]
	eta	$[2^{-10}, 1.0]$
	max_depth	[1, 50]
	reg_lambda	$[2^{-10}, 2^{10}]$
RandomForest	max_depth	[1, 50]
	max_features	[0.0, 1.0]
	min_samples_leaf	[1, 2]
	min_samples_split	[2, 128]
MLP	alpha	$[1.0e^{-08}, 1.0]$
	batch_size	[4, 256]
	depth	[1, 3]
	learning_rate_init	$[1.0e^{-05}, 1.0]$
	width	[16, 1024]

formity in the quality and detail of evaluations, focusing on achieving precision with every iteration. The outcomes of these benchmarks reveal `HomOpt`'s robust capabilities in managing complex hyperparameter optimization tasks and highlight its performance benefits over traditional methods, even without leveraging multiple levels of fidelity. The configuration spaces for the NAS benchmarks can be found in Table 4.

Table 4: Configuration space for the NAS-Bench-201 benchmark on CIFAR-10 and ImageNet16-120.

Component	Type	Choices / Range
Edge 0	Categorical	{none, skip_connect}
Edge 1	Categorical	{none, skip_connect, nor_conv_1x1, nor_conv_3x3}
Edge 2	Categorical	{none, skip_connect, nor_conv_1x1, nor_conv_3x3, avg_pool_3x3}
Edge 3	Categorical	{none, skip_connect, nor_conv_1x1, nor_conv_3x3, avg_pool_3x3}
Epochs	Integer	[12, 200]

4.1 Evaluation Criteria

For the HPOBench classification benchmarks on popular ML algorithms, the optimizer performance is evaluated based on the validation performance (*i.e.*, the objective value seen by the optimizer). This objective value was minimized over $1 -$ accuracy and a summary across all of the benchmark experiments are reported. Additional results including the corresponding values for test scores are included for each experiment in Appendix A.

In the evaluation of optimization methods within our HPOBench ML experiments, we employ the *simple regret* as a performance metric. Simple regret measures the gap between the best loss value that a method has achieved by iteration t and the best observed loss value across all methods and benchmarks. It is defined for iteration t as:

$$R_t = \min_{i=1}^{t} f(x_i) - f(x^*) \tag{7}$$

where R_t signifies the simple regret at iteration t, $\min_{i=1}^{t} f(x_i)$ denotes the lowest loss value secured by the method up to that point, and $f(x^*)$ represents the lowest loss value found among all trials and methods across the given benchmarks. This best observed value serves as an approximation of the global minimum when the true optimal solution is unknown. Lower values of R_t indicate a performance closer to this best found solution, reflecting improved effectiveness of the optimization method. Conversely, higher values suggest a greater deviation from the optimal performance. For enhanced visual discernment, regret is plotted on a logarithmic scale. The goal is to minimize simple regret; thus, a downward trend in the regret plot is desirable, as it indicates progressive improvement in optimization performance.

For the open-set experiments, the trained EVM is optimized to minimize the loss on a validation set of data containing samples from both known and unknown classes within the number of search trials listed in Table 5. This loss is defined as the negative $F1$ score with *weighted* averaging:

$$F1 = \frac{2 \cdot \text{Precision} \cdot \text{Recall}}{\text{Precision} + \text{Recall}} = \frac{2 \cdot \text{TP}}{2 \cdot \text{TP} + \text{FP} + \text{FN}} \tag{8}$$

where TP, FP, and FN are the number of true positives, false positives, and false negatives, respectively. The negative $F1$ score used as the loss function for optimization is defined as:

$$\text{Negative } F1 = -F1 \tag{9}$$

Minimizing the negative $F1$ score effectively aims to maximize the F1 score, as a higher F1 score indicates better model performance.

In evaluating `HomOpt` on NAS tabular benchmarks, we focus on the median optimized regret as a key performance metric. This metric provides insight into the effectiveness of the optimization strategy by measuring the difference between the function value of the incumbent (best observed configuration) and the global optimum over time. For our analysis, we specifically report results based on version 2 (v2) of the trajectory evaluation criteria, which prioritizes configurations purely based on their function value, disregarding the budget or computational resources used to obtain them. This approach aligns with our goal to assess the raw optimization capability of the methods in identifying high-performing configurations as efficiently as possible.

The choice of v2 over version 1 (v1) is motivated by the nature of `HomOpt` as a hyperparameter optimization method rather than a multi-fidelity optimizer. Unlike multi-fidelity approaches

that strategically allocate resources across different levels of budget to expedite the search process, `HomOpt` focuses on navigating the hyperparameter space within a single fidelity. In this context, v2's disregard for budget in determining incumbents allows us to directly compare the intrinsic optimization performance of `HomOpt` against other methods without the confounding effects of budget management.

4.2 Experimental Setup

`HomOpt` can be used to augment any base HPO strategy. We thus compare the performance boost of `HomOpt` with GAM surrogates against the base performance of common popular hyperparameter optimization approaches: Random Search, Bayes, TPE, and SMAC. The numbers of iterations and samples used in the different optimization methods were chosen based on previous empirical experiments and theoretical considerations to balance the trade-off between the computational cost and the expected performance of the method. With TPE we used 20% of the results for the top-k mixture model seeded with 10 random search iterations and 10 generated candidates samples. In the Bayes examples, we used 20 random search iterations with 10 candidate samples. And for the SMAC runs, we used 20 random search iterations with 20 candidate samples. `HomOpt` similarly was initialized with 20 evaluations ($\mathcal{W} = 20$) from each of the base strategies.

All experiments were run for 500 iterations across 5 separate seeds and averaged together. The HPOBench classification experiments were run on a multitude of dataset tasks from OpenML (Vanschoren et al., 2014), which is open platform for sharing datasets, and the open-set experiments were conducted on the handwritten digits dataset MNIST (Deng, 2012) and Labeled Faced in the Wild (LFW) (Huang et al., 2007).

For the open-set experiments, we chose MNIST and LFW to consider two datasets of different complexity and modified each classification task to convert from a closed-set task to an open-set one. Table 5 summarizes the dataset experiments in terms of number of search trials, number of known and unknown classes, and number of training, validation, negatives, and testing samples. Negatives are samples from the unknown class without labels used to better inform the "1 vs. rest" classifiers when training the EVM. The number of trials for each experiment was determined and adjusted according to the time required to train a single model for the given dataset. If the dataset contained many images per class, fitting the EVM to the feature vectors for large samples required longer compute time and thus the number of search trials was reduced.

Experiment	# Search Trials	# Known Classes	# Unknown Classes	Training	Validation	Negatives	Testing
MNIST	1000	6	4	28824	12000	19176	10000
LFW	1000	34	5715	1333	2481	6110	3309

Table 5: Summary of dataset characteristics for open-set experimental sets.

For the handwritten digits dataset MNIST, we designate handwritten digits 0 to 5 as the known classes and digits 6 to 9 as the unknown. Each image is represented as a flattened vector of the image pixels (784 features). For Labeled Faces in the Wild (LFW), we use classes with 30 or more face image samples to designate the known classes (34) and assign the remaining classes (5715) as the unknown set. The network used to extract features is an ArcFace (Deng et al., 2022) based feature extractor (Albiero et al., 2020) trained on the MS-Celeb-1M dataset (Guo et al., 2016) resulting in a 512 dimensional feature vector.

Threshold, cover threshold, and distance multiplier are sampled from a uniform distribution of range $[0, 1]$. The fitting algorithm for the EVM requires that the tailsize not exceed greater than half the number of training samples. For this reason, the tailsize hyperparameter was sampled from a uniform distribution between the range $[0, 0.5]$ and used as a multiplier to determine how many negative samples were included in estimating the model parameters.

Our default values for the parameters in the experiments were values found to be effective in empirical studies on simple problems and common choices found in literature. For all experiments, the distance threshold $\mathcal{D}$ is computed by the variance of the best 10% of the observed sample points scaled by 0.005 (also known as the jitter strength) as the local perturbation search around the observed minimum in Algorithm 1. In all the experiments we use 5 iterations which are the number of minimizations to compute the homotopy ($\mathcal{N}$). This strikes a balance between the computational costs and finding a good solution. Fewer iterations may not find a good solution, while more iterations may be computationally expensive without much benefit in terms of improved performance. We use a k of 0.5 which are the fraction of complete trials used to train one of the GAMs. Using half the completed trials provides a good balance between using enough data to train the model and not overfitting to the data. A smaller value of k would mean the GAM is trained on fewer data points, which may result in underfitting. A larger value of k would mean the GAM is trained on more data points, which may result in overfitting. The GAM model surrogates use a penalty term on the smooth functions of 10^{-4} and 25 splines for all experiments. The penalty term helps to control the complexity of the surrogate model. A smaller penalty term would result in a model that fits the data well but is likely to overfit. A larger penalty term would result in a model that is less likely to overfit but may not fit the data as well. Similarly, fewer splines would result in a simpler model that is less likely to overfit but may not fit the data as well, while more splines would result in a more complex model that fits the data well but is likely to overfit.

In our experiments, we have search domains that consist of both discrete and categorical hyperparameters. To perform optimization on these domains, we first cast each hyperparameter to its corresponding index in an array. Then, we convert these indices to floating-point numbers so that we can use continuous optimization algorithms. Finally, we round the output of the optimization algorithm to the nearest index to get the final hyperparameter configuration. This allows us to use continuous optimization algorithms on search domains that consist of discrete and categorical hyperparameters.

The NAS tabular benchmarks uses CatBoost models as surrogates within the `HomOpt` framework. We use the same setup on both CIFAR-10 and ImageNet16-120. For each trial, based on the accumulated trial data, the algorithm decides whether to sample a new configuration randomly (during the warm-up phase) or proceed with the optimization process. We again set the warm-up phase to 20 trials and upon transitioning to optimization, the algorithm employs two distinct CatBoost models: one for exploration and one for exploitation, each trained with 1000 iterations. The exploration model is trained on a broader dataset to identify unexplored regions with potential, while the exploitation model focuses on refining the search around previously identified promising areas. The exploitation model, in particular, is trained on the top configurations determined by sorting the trial data by loss and selecting the best performers. The selection criterion dynamically adjusts to consider at least 5 configurations or a proportion (20%). The core of the optimization process is the homotopy optimization loop, consisting of 100 steps. This loop gradually transitions the focus from exploration to exploitation by adjusting the homotopy parameter t from Algorithm 2 from 1

(pure exploration) towards 0 (pure exploitation). This strategic modulation allows the algorithm to leverage the strengths of both strategies over the course of the optimization process.

We compare `HomOpt` against the following optimization techniques for the NAS benchmarks:

- **Hyperband enhanced with Bayesian Optimization (BOHB)**: Merges the rapid configuration assessment capabilities of Hyperband with the probabilistic modeling strength of TPE, optimizing the exploration and exploitation of the search space (Falkner et al., 2018).
- **Random Search (RS)**: Employs a straightforward and unbiased approach by uniformly sampling the hyperparameter space, serving as a baseline for evaluating the efficiency of more complex methods (Bergstra and Bengio, 2012b).
- **Bayesian Optimization with Kernel Density Estimators (BO-KDE)**: Leverages kernel density estimators to model the probability distribution of effective hyperparameters, refining the search strategy over successive iterations (Bergstra et al., 2011b).
- **Optuna with Median Stopping Rule (Optuna$^{\text{med_tpe}}$)**: Integrates TPE with a median stopping rule, which prunes less promising trials early, enhancing computational efficiency (Golovin et al., 2017).
- **Optuna Variants for Enhanced Sampling**:
  - **Optuna$^{\text{hb}}$**: Adapts Hyperband's resource allocation strategy to work with TPE, focusing on accelerating convergence towards optimal configurations.
  - **Optuna$^{\text{rs}}$**: Combines the benefits of TPE with the straightforward, unbiased approach of random search, offering a balanced exploration method.
- **Optuna's Tree-structured Parzen Estimator (Optuna$^{\text{tpe}}$)**: Utilizes Gaussian Mixture Models for probabilistically guiding the search towards regions of the hyperparameter space likely to yield better performance (Akiba et al., 2019).

4.3 Results

4.3.1 HPOBench Classification Experiments

We compare the performance of `HomOpt` on the tuning of different sets of parameters on the SVM, Random Forest, Logistic Regression, MLP and XGBoost benchmarks from the HPOBench suite across multiple dataset tasks from the OpenML library. In all these experiments we use the same parameters for `HomOpt` across all benchmarks and datasets. Figures 6 - 10 reflect the regret at each iteration for all the ML benchmarks. The regret plots illustrate the difference between the performance at each iteration compared to the best value found for the entire dataset. Thus, the lower the regret, the better the optimization algorithm is performing. A summary of the performance on the best observed validation accuracy is additionally included in Appendix C.1.1 where we see an improvement in minimizing the validation loss for a majority of the datasets in 4 of the 5 benchmarks.

In the Random Forest benchmark shown in Figure 6, for each of the 13 datasets, we can see a consistent trend where `HomOpt` successfully improves the performance of all the base methods alone where the regret plots demonstrated a faster convergence to a better optima. The trials where

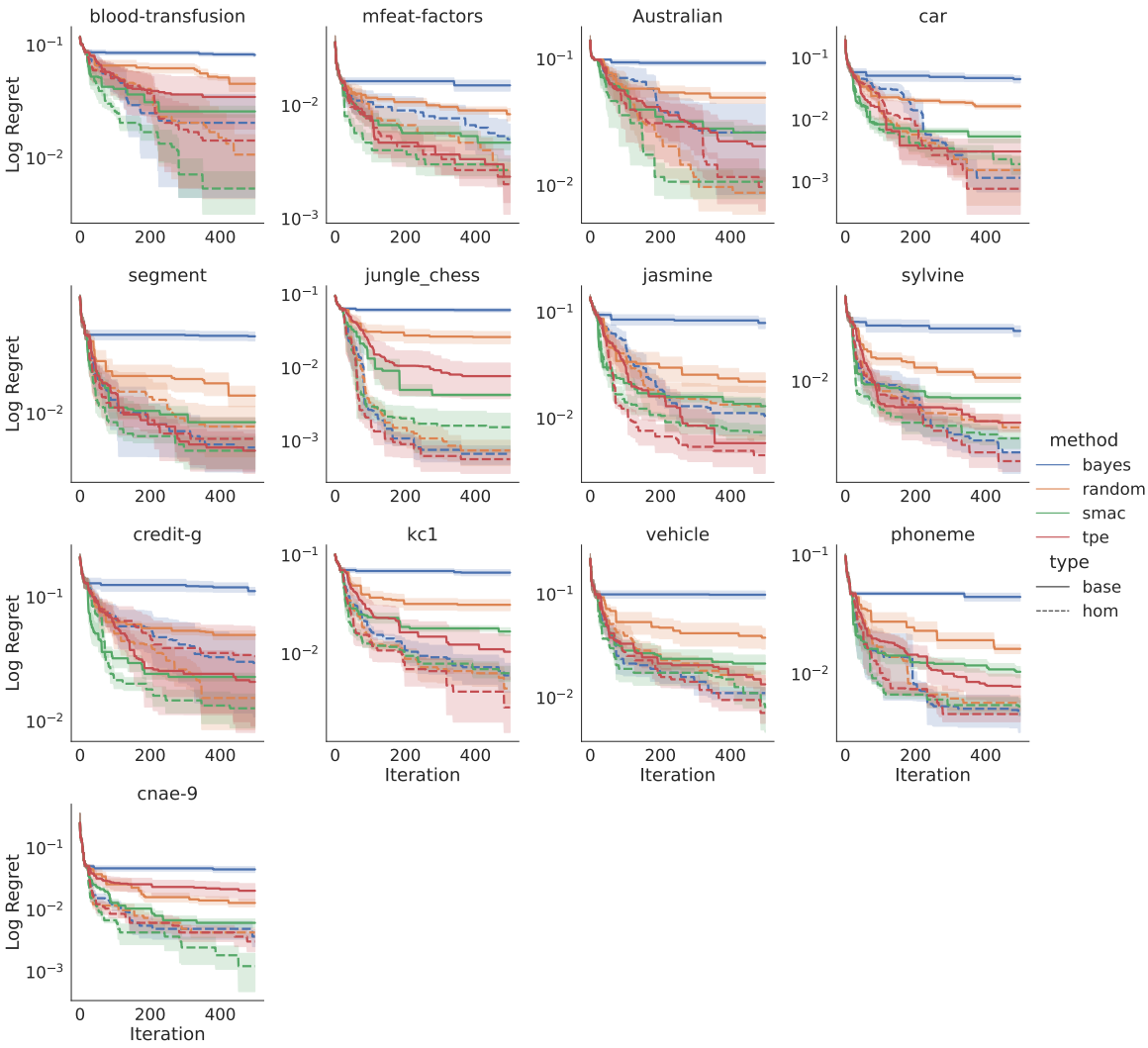

Figure 6: Comparison of all methods on 13 different tasks for the Random Forest Benchmark from the HPOBench suite. The mean and standard error of the regret at each iteration are displayed across 5 repetitions.

HomOpt augmented the base methodologies are indicated with the dashed line which have steeper slope compared to the base methods alone (indicated by the solid lines). Each of the datasets had varying number of instances and features as indicated in Table 2. The most significant improvement of HomOpt over the base methods can actually be seen in the dataset with the highest number of features but relatively low number of instances (cnae-9). Random Forest has four hyperparameters (Table 3), and although the ranges may not be too wide, the combination and interaction of this space can make it challenging. The min_samples_leaf and min_samples_split hyperparameters have relatively narrow ranges, but the interaction between these hyperparameters and max_depth can make the search space challenging. For example, setting min_samples_leaf or min_samples_split too small can lead to overfitting, especially when max_depth is also large. On the other hand, setting these hyperparameters too large can lead to underfitting, especially when max_depth is small.

Compared to the Random Forest benchmark, the SVM benchmark illustrated in Figure 7 consists of only two hyperparameters, leading to a lower dimensionality in its search space. However, the search space for SVM is more extensive than that of the Random Forest benchmark, as both hyperparameters (C and gamma) have a range spanning from 2^{-10} to 2^{10}. These ranges are significantly large, covering several orders of magnitude, which poses a challenge when navigating through the search space. HomOpt demonstrates a relative boost over the base methodologies regarding in specific datasets such as the Australian, car, segment, jasmine, sylvine, and vehicle datasets. On the other hand, in datasets like blood-transfusion, mfeat-factors, credit-g, kc1, and cnae-9, the results across all methods, including those augmented with HomOpt, are relatively similar. The search space in these datasets may contain complex interactions between hyperparameters, making it difficult for all methods to find the optimal configurations. Consequently, the convergence to the optimum in these cases may not be as significant when compared to the base methodologies for these datasets. While HomOpt with the default parameters demonstrates an overall boost in many of the datasets concerning the overall optima, the convergence to the optimum is not as pronounced. In several cases, the results are comparable or only marginally better than the base methodologies. This suggests that HomOpt might offer advantages in specific scenarios, but its performance may be influenced by a combination of factors, such as the inherent complexity of the datasets, the optimization algorithm's ability to navigate the search space, and the interactions between hyperparameters in the SVM benchmark.

The search space for the Logistic Regression benchmark is relatively straightforward, consisting of only two hyperparameters: alpha and eta0. These hyperparameters have a range of 1e-05 to 1.0, which is notably smaller compared to the broader ranges observed in SVM's hyperparameters. This simpler search space allows for more manageable exploration and optimization, as it does not involve as many complex interactions between hyperparameters as seen in other benchmarks. The impact of HomOpt on the Logistic Regression benchmark (Figure 8) exhibits a trend similar to the results observed in the Random Forest benchmark. In both cases, the trials incorporating HomOpt demonstrate an overall improvement in performance across all 20 datasets. Additionally, HomOpt facilitates a faster convergence towards a lower optimal value, suggesting that the optimization algorithm is more efficient in navigating the search space and identifying better hyperparameter configurations than the base methodologies alone. This improved performance of HomOpt in the Logistic Regression benchmark can be attributed to several factors. The relatively simple search space, with fewer hyperparameters and a smaller range, enables a more effective exploration of possible configurations. Additionally, the inherently lower complexity of the Logistic Regression model, compared

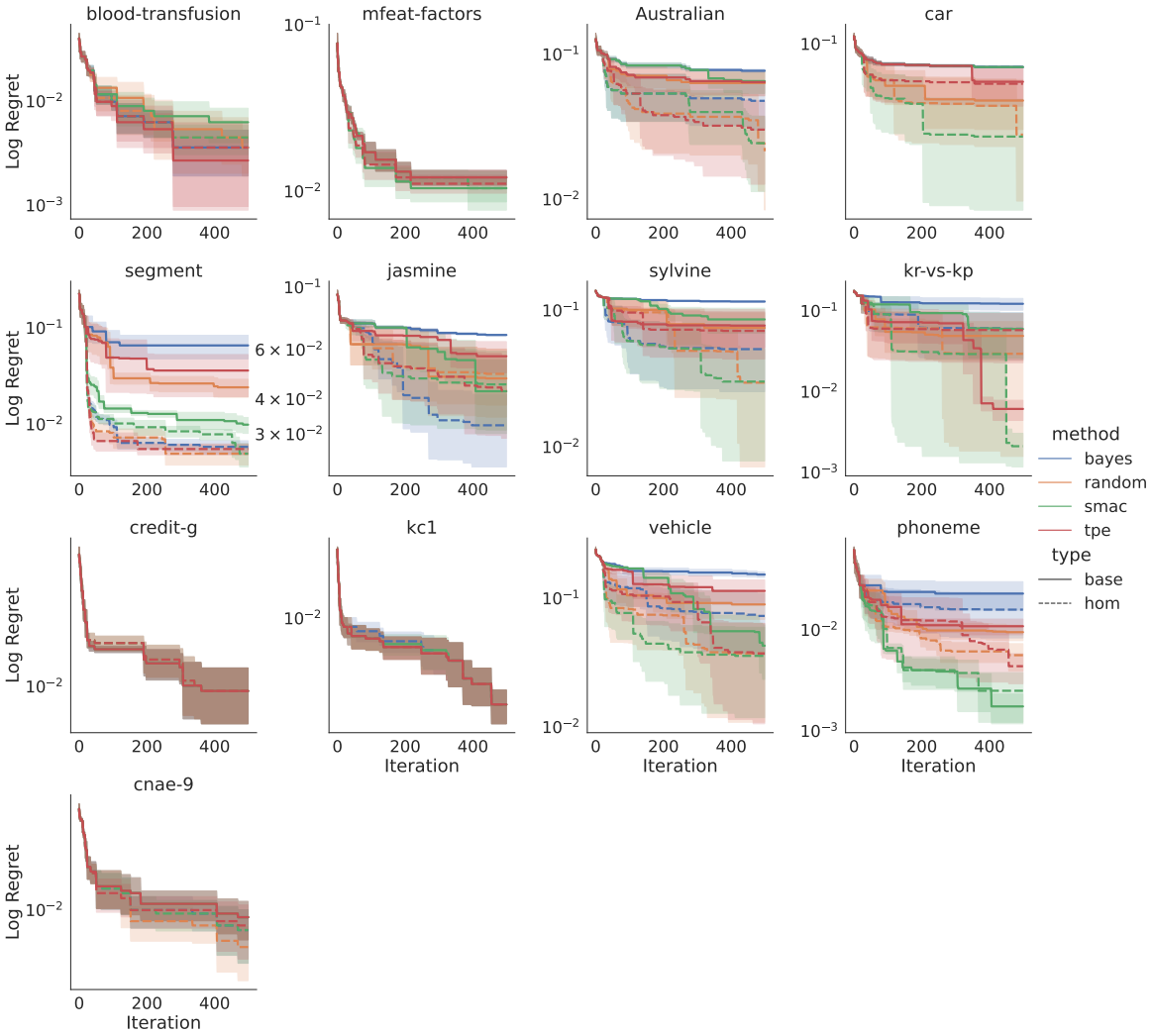

Figure 7: Comparison of all methods on 13 different tasks for the SVM Benchmark from the HPOBench suite. The mean and standard error of the regret at each iteration are displayed across 5 repetitions.

to models with larger search spaces or more hyperparameters, could also contribute to the improved performance observed when using `HomOpt`.

The MLP model has a larger search space with its five hyperparameters, leading to a greater number of possible configurations. The interactions between these hyperparameters are quite complex, further contributing to the challenge of optimizing this model. For instance, the depth and width of the network directly impact its capacity and complexity, while the alpha (L2 regularization) and learning_rate_init parameters control the model's generalization performance. Additionally, the batch_size parameter influences not only the convergence speed but also the quality of the final solution. Navigating these intricate interactions within the MLP search space can be extremely challenging for HPO algorithms. Despite these challenges, `HomOpt` has demonstrated a significant boost in performance compared to the base methodologies in 5 different datasets (Figure 9). This

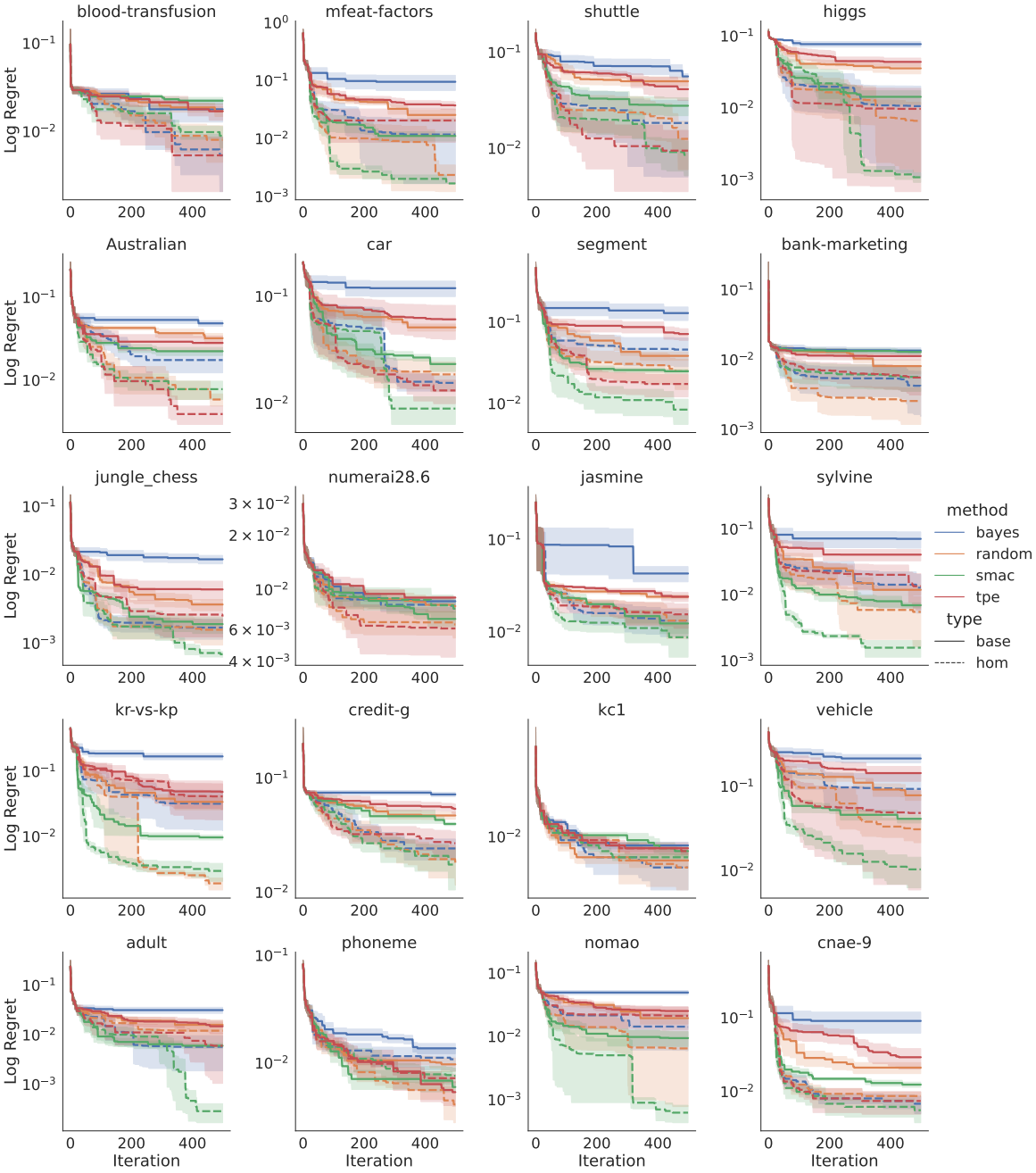

Figure 8: Comparison of all methods on 20 different tasks for the Logistic Regression Benchmark from the HPOBench suite. The mean and standard error of the regret at each iteration are displayed across 5 repetitions.

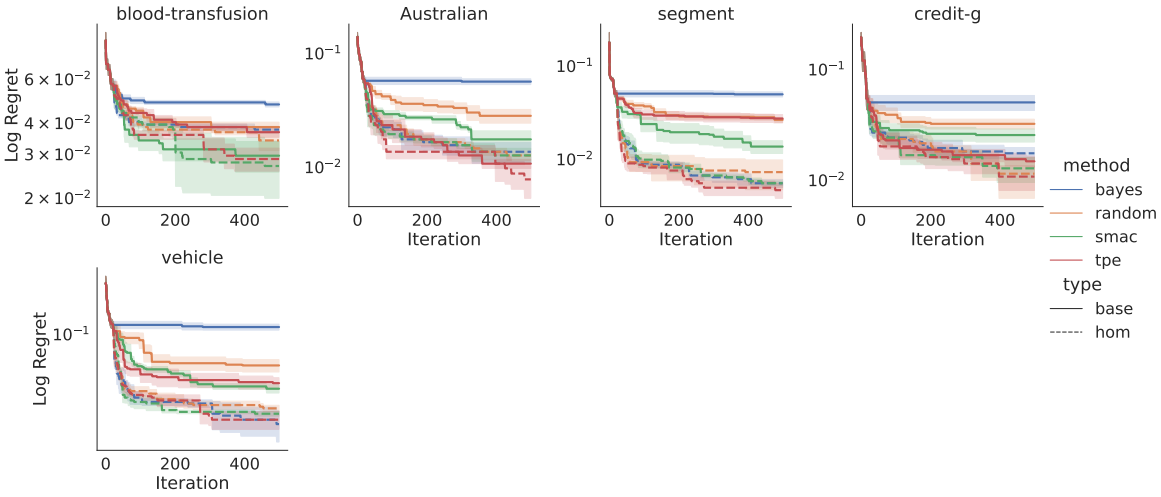

Figure 9: Comparison of all methods on 5 different tasks for the MLP Benchmark from the HPOBench suite. The mean and standard error of the regret at each iteration are displayed across 5 repetitions.

improvement is evidenced by lower optimal scores and faster convergence rates. Furthermore, the standard error of the regret in the MLP benchmark is consistently lower than that of the SVM benchmark across the five repetitions. This suggests that the optimization process for MLP is more stable and less prone to random fluctuations compared to SVM. This could be attributed to the fact that the MLP search space is more constrained compared to SVM due to the smaller range of hyperparameters, resulting in a more focused search. This, in turn, could lead to a more stable optimization process with a more prominent boost in the performance.

XGBoost has four hyperparameters: colsample_bytree, eta, max_depth, and reg_lambda. The search space complexity is higher than that of SVM and Logistic Regression due to the increased number of hyperparameters. The ranges of these hyperparameters are quite different, with some having smaller ranges (e.g., colsample_bytree) and others having larger ranges (e.g., max_depth and reg_lambda). Among all five of the benchmarks from HPOBench, `HomOpt` demonstrated the least noticeable improvement in the XGBoost experiments[3]. As seen by the regret plots in Figure 10 the results among all the methods appeared to have a similar effect in regards to the convergence and the overall optimum. We can see a small boost in performace for random and bayes with `HomOpt` in the blood-transfusion dataset which has only 4 features and 748 instances but otherwise a noticeable boost can not be seen. One possible reason why `HomOpt` did not perform as well on the XGBoost benchmark compared to the other benchmarks could be due to the interactions between the four hyperparameters. The interactions may be more intricate and complex compared to the other benchmarks, making it more challenging for `HomOpt` to effectively explore the search space and find the optimal solution. These hyperparameters are also interdependent with each other. For instance, a higher eta value may require a higher reg_lambda value to counteract the increased learning rate. The ranges of the hyperparameters in XGBoost vary widely. For example, the colsample bytree parameter has a range of [0.1, 1.0], while the max_depth and reg_lambda parameters have

3. We include a study into the meta-parameters for this benchmark in the supplemental material (Section A.1)

ranges of [1, 50] and $[2^{-10}, 2^{10}]$, respectively. This heterogeneity in the ranges could also contribute to the difficulty of exploring the search space efficiently.

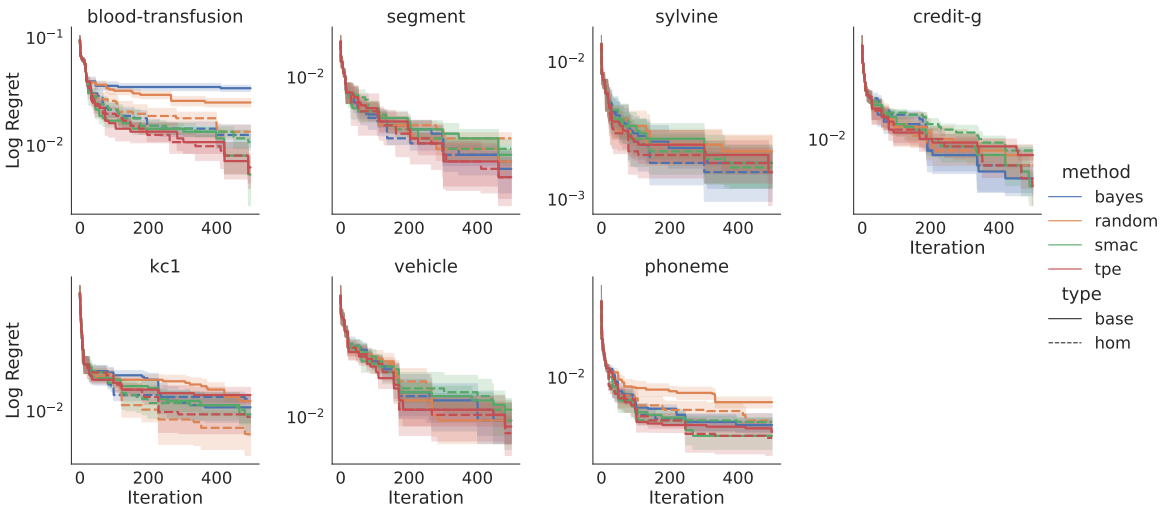

Figure 10: Comparison of all methods on 14 different tasks for the XGBoost Benchmark from the HPOBench suite. The mean and standard error of the regret at each iteration are displayed across 5 repetitions.

4.3.2 Open-Set Benchmarks

Optimizing the EVM model can be challenging due to the complexity of its hyperparameters and the high-dimensional nature of the data it handles. The EVM algorithm has five hyperparameters, each with its own domain and range, which must be tuned to achieve optimal performance. The tailsize parameter, in particular, can be difficult to optimize, as it determines the number of negative samples used to estimate the model parameters. This parameter can have a significant impact on the model's performance, but it is also highly dependent on the characteristics of the input data. Additionally, the distance function parameter can be difficult to optimize because it affects the way the model computes distances between samples, and this can have a significant impact on the model's accuracy. Finding the right combination of hyperparameters to optimize the EVM model can be a time-consuming and challenging task for any HPO algorithm. In Figure 11, we evaluate the performance of `HomOpt` in tuning the 5 hyperparameters of an open-set recognition algorithm, the EVM on two separate datasets over 5 random seeds. `HomOpt` again demonstrates a faster convergence to a better optimum value for both datasets, boosting all of the methods that were tested and also on average found a better objective value (observed $F1$ score). Compared to some of the other models in HPOBench, the EVM has a relatively small and constrained hyperparameter search space. The threshold, tailsize, cover threshold, and distance multiplier parameters all have ranges between 0 and 1, while the distance function is limited to two options: Cosine or Euclidean distance. This limited search space may partially explain why `HomOpt` was able to perform well on the EVM benchmark.

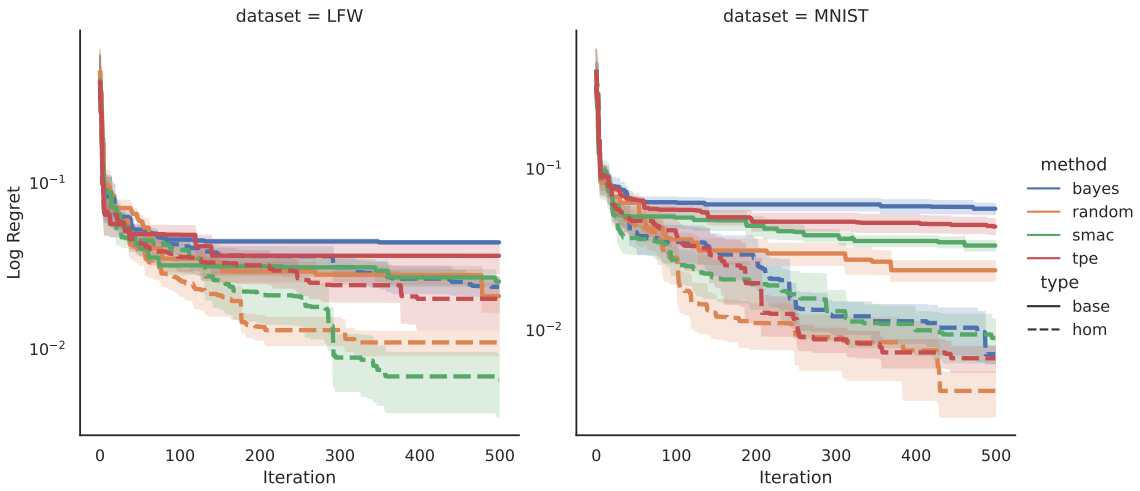

Figure 11: Comparison of all methods on MNIST and LFW for the open-set benchmarks. The mean and standard error of the regret at each iteration are displayed across 5 repetitions. `HomOpt` *boosts the performance of all the methods for both of the datasets.*

4.3.3 NAS-BENCHMARKS

The empirical evaluation of `HomOpt` on the CIFAR-10 benchmark provides additional perspectives on its optimization capabilities, especially when compared to traditional black-box and state-of-the-art multi-fidelity methods. The utilization of surrogate models, coupled with homotopy-based optimization techniques, allows `HomOpt` to effectively exploit high-fidelity evaluations, achieving good performance with the smallest number of function calls among the tested optimizers. This is reflected in Table 6 by `HomOpt`'s low actual worst-case time (act_wc_time) and an initial sharp decline in median optimized regret shown in the associated figures (Figure 12a).

Table 6: Comparative analysis of average performance metrics for various hyperparameter optimization methods applied on the Cifar 10 benchmark. The table includes average wall-clock time for actual runs (act_wc_time) in seconds, the difference in wall-clock time from the fastest method (diff_wc_time) in seconds, the number of function calls (n_calls), and the simulated wall-clock time (sim_wc_time) in seconds. This comprehensive overview allows for a direct comparison of efficiency and speed among methods, highlighting `HomOpt`*'s competitive performance in terms of speed and number of evaluations required.*

Optimizer	act_wc_time	diff_wc_time	n_calls	sim_wc_time
`HomOpt`	12857.8	9.15614e+06	200	843861
$\text{BOHB}_{\text{eta2}}$	117634	26006.7	3914.5	9.97399e+06
BOHB	99333.2	3554.43	3149.59	9.99645e+06
BO_{KDE}	38644.6	4753.34	1303.84	9.99525e+06
$\text{Optuna}_{\text{RS}}$	43463.7	3585.54	1363.11	9.99641e+06
$\text{Optuna}^{\text{hb}}_{\text{TPE}}$	212687	2054.04	5525.86	9.99795e+06
$\text{Optuna}^{\text{med}}_{\text{TPE}}$	83264.5	3370.23	2852.06	9.99663e+06
RS	41791.9	95544.2	1351.45	9.90446e+06

Despite its strengths in quickly navigating the search space, HomOpt exhibits a relatively high differential worst-case time (diff_wc_time), suggesting performance variability across runs. While this may be a concern in scenarios demanding consistent outcomes, it is worth noting that such variability could stem from the complex landscapes of deep learning optimization tasks, where even subtle changes in hyperparameters can lead to vastly different model performances.

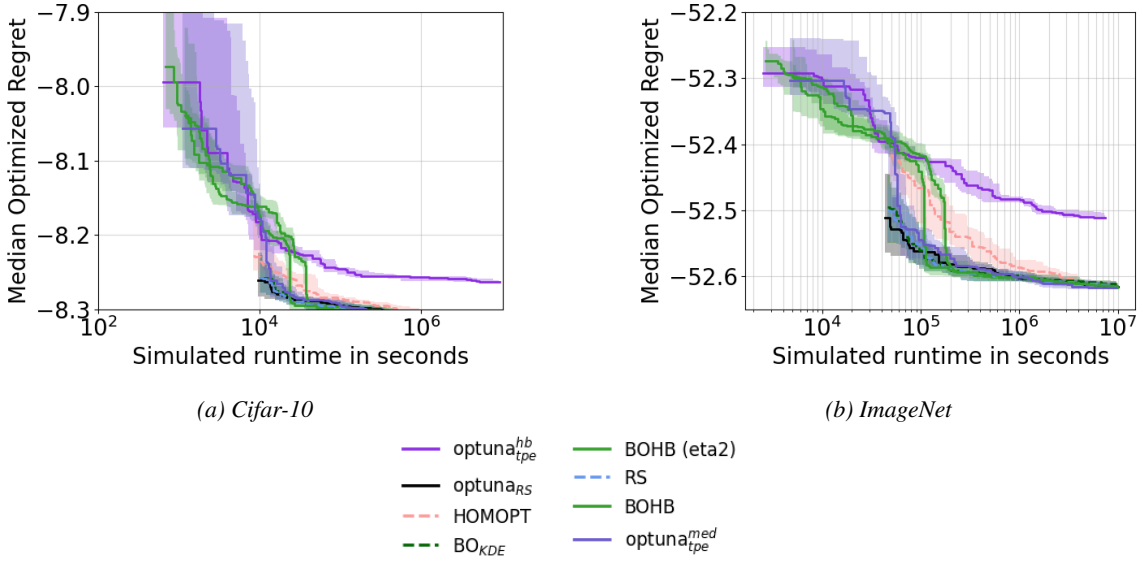

(a) Cifar-10 *(b) ImageNet*

Figure 12: Comparison of median optimized regret across simulated runtimes for different hyperparameter optimization techniques on NAS benchmarks. The graphs display results for HomOpt in pink and other contemporary methods. The performance on Cifar-10 (left) and ImageNet (right) demonstrates HomOpt's efficiency, showing a fast convergence towards lower regret values, particularly evident in the Cifar-10 benchmark. The shaded regions represent the interquartile range across multiple trials, highlighting the consistency and reliability of HomOpt's in different experimental settings.

HomOpt primarily uses high-fidelity evaluations, which are detailed and accurate assessments of model performance. This approach does not prioritize the quick, less detailed evaluations seen in multi-fidelity methods, which can sometimes lead to computational savings. By focusing exclusively on high-fidelity evaluations, HomOpt ensures that every evaluation provides deep insights into the optimization landscape, minimizing the risk of being misled by the less accurate results of lower-fidelity evaluations. Over time, this method helps HomOpt consistently find the best solutions, maintaining strong performance even in challenging scenarios.

To further enhance HomOpt's efficacy, particularly in maintaining performance improvements over extended periods, an integration of dynamic adaptation strategies could be instrumental. Borrowing from the principles of multi-fidelity methods, HomOpt could implement a semi-multi-fidelity approach that incorporates surrogate-assisted low-fidelity evaluations to guide the homotopy transformations. Such a strategy would not only mitigate the observed performance variability but also enrich the exploration phase, thereby reinforcing HomOpt's capacity for sustained optimization. Moreover, augmenting HomOpt with adaptive resource allocation could refine its long-term performance consistency. By progressively focusing computational efforts on promising regions of the search space, as indicated by the surrogate model's insights, HomOpt can balance exploration and exploitation more effectively.

Table 7: Comparative analysis of average performance metrics for various hyperparameter optimization methods applied to the ImageNet benchmark. This table quantifies each method's actual wall-clock time (act_wc_time) in seconds, the difference in wall-clock time from the fastest method (diff_wc_time) in seconds, the number of function calls (n_calls), and the simulated wall-clock time (sim_wc_time) in seconds. Notably, `HomOpt` *demonstrates competitive efficiency with significantly lower wall-clock time and fewer function calls compared to other methods, emphasizing its optimized performance for large-scale datasets like ImageNet.*

	act_wc_time	diff_wc_time	n_calls	sim_wc_time
`HomOpt`	13976.69	6.022e+06	200	3.978396e+06
$\text{BOHB}_{\text{eta2}}$	31056.87	1.347e+04	894.28	9.987e+06
BOHB	22548.32	1.374e+04	718.84	9.986e+06
BO_{KDE}	10371.78	1.639e+04	298.37	9.9836e+06
$\text{Optuna}_{\text{RS}}$	8964.93	1.584e+04	297.82	9.984e+06
$\text{Optuna}^{\text{hb}}_{\text{TPE}}$	36041.43	7.283e+03	1101.5	9.993e+06
$\text{Optuna}^{\text{med}}_{\text{TPE}}$	17203.68	1.525e+04	538.85	9.985e+06
RS	9942.98	1.593e+04	298.10	9.984e+06

On the ImageNet benchmark, `HomOpt` continues to demonstrate a similar trend of efficient convergence (Figure 12b) with the lowest number of function calls (Table 7). Its actual worst-case time (act_wc_time) remains competitive, and the simulated worst-case time (sim_wc_time) is notably the lowest among all methods, reinforcing `HomOpt`'s effectiveness in challenging conditions. Again, `HomOpt` exhibits a relatively high differential worst-case time (diff_wc_time), suggesting performance variability across runs on both benchmarks. In Figure 12 we can see `HomOpt` is able to eventually converge to an optimal and maintain raw competitive performance even against its multi-fidelity counterparts.

It's important to note that while `HomOpt` does not inherently leverage multi-fidelity techniques, its efficiency and effectiveness in identifying optimal or near-optimal configurations demonstrate its robustness as an optimization tool. This focus on pure optimization performance, as captured by the median optimized regret under v2 criteria, underscores `HomOpt`'s potential to enhance hyperparameter search processes across a range of computational budgets and resource constraints.

5. Limitations

Despite `HomOpt`'s strong performance across a range of benchmarks, it's important to acknowledge the framework's reliance on surrogate models—namely in this work, Generalized Additive Models (GAM) and CatBoost—brings forth certain limitations. Surrogate models, while designed to reduce the computational overhead typically associated with direct evaluations in methods like Bayesian Optimization, do introduce their own complexities. These include the computational cost associated with constructing and updating the models, and the necessity for precise tuning of their hyperparameters to align with the objective function's characteristics. Misalignment or inadequate tuning can result in suboptimal optimization paths.

Furthermore, `HomOpt`'s current framework is highly efficient at exploiting well-understood regions of the search space, yet it may lack robust mechanisms for broader exploration, particularly in vast or complex hyperparameter spaces. This limitation may prevent `HomOpt` from identifying diverse global solutions or adapting quickly to new optimization landscapes, which are critical

in dynamic environments. Enhancing HomOpt's exploration capabilities could involve integrating strategies that promote greater diversity in the search process, such as periodic resets or incorporating elements of randomness in the choice of surrogate models.

To enhance the robustness of the optimization process, adopting a strategy that leverages multiple surrogate models or integrates assessments of model uncertainty could prove beneficial (Hutter et al., 2019). For this study, our utilization of GAM and CatBoost as surrogates was deliberate; GAMs were chosen for their interpretability and flexibility, allowing for a nuanced understanding and adjustment of the relationship between hyperparameters and the optimization objective. Our GAM configuration employed a penalty term of 10^{-4} on the smooth functions and used 25 splines, aiming to balance complexity and overfitting risks. CatBoost, on the other hand, provided a gradient boosting framework that excels in handling categorical features and complex data relationships, complementing the GAM's capabilities.

While HomOpt demonstrates configurability as a strength, selecting the optimal settings for both the framework itself and its surrogate models' hyperparameters presents a challenge. Ablation studies highlighted this, underscoring the sensitivity of optimization outcomes to these settings. Future iterations could benefit from employing adaptive strategies, such as reinforcement learning (Sutton and Barto, 2018), to dynamically tune these meta-parameters, mitigating the trial-and-error approach. Alternatives to GAM and CatBoost, including random forests (Breiman, 2001), Bayesian networks (Ghahramani, 2006), and other gradient boosting machines (Friedman, 2001), offer further avenues for exploration. Though beyond this paper's scope, such alternatives promise adaptability to diverse problem settings (Bhosekar and Ierapetritou, 2018).

The computational efficiency and scalability of HomOpt are contingent upon the chosen surrogate model's complexity. While this may limit its applicability in large-scale, distributed computing environments compared to simpler strategies, leveraging parallel surrogate model training and evaluation could ameliorate these constraints (Kandasamy et al., 2018). Furthermore, the efficacy of HomOpt hinges on the quality and diversity of the training data for the surrogate models. Incorporating active learning or transfer learning principles could augment data efficiency, mitigating this limitation and potentially enhancing optimization performance across varied domains (Settles, 2009; Pan and Yang, 2009).

In the current configuration of HomOpt, only one optimal point is found. However, this can be modified by utilizing a different surrogate which tracks the change of multiple minima at spread out regions. This can also be modified by taking the number of points within the top $\alpha\%$ instead of utilizing a single point. We also consider the adaption of HomOpt for other applications key to hyperparameter optimization such as incorporating domain knowledge. HomOpt provide a framework integrating the the use of homotopies to track the transition between minimums which can enable the incorporation of domain knowledge in the form of constraints or heuristics that better guide the optimization process.

Additionally, while the continuous deformation between models underpins HomOpt's thorough exploration capabilities, addressing irregular or noisy objective functions may require adaptive homotopy paths or integrating derivative-free optimization techniques for improved convergence (Rios and Sahinidis, 2013).

As we continue to refine HomOpt, we are optimistic about its potential to streamline the hyperparameter optimization process. By incorporating advanced strategies such as adaptive homotopy paths and exploring alternative surrogate models, HomOpt can become even more versatile and

powerful. These future directions promise to mitigate the limitations observed while maximizing the strengths of this framework.

6. Conclusion

We introduced `HomOpt` an advanced HPO framework that introduces the use of continuous deformation between surrogate models, coupled with homotopy methods, to adeptly navigate the hyperparameter space. This innovative approach facilitates the tracking of local minima across evolving surrogate landscapes, thereby pinpointing critical regions of interest with unprecedented efficiency. `HomOpt` not only expedites the convergence towards optimal solutions but also harmonizes with a variety of established HPO methodologies, enhancing their performance by achieving faster convergence and uncovering performant solutions in a multitude of benchmark scenarios. These benchmarks span a diverse array of optimization challenges, underscoring the comprehensive nature of our evaluation and the methodological rigor of `HomOpt`.

Significantly, `HomOpt`'s design philosophy embodies versatility, allowing for seamless integration with any HPO approach and showcasing marked improvements in convergence speeds across both well-defined and more exploratory model settings, all while maintaining a minimal set of assumptions about the objective function's behavior. Looking ahead, we are hope to broaden `HomOpt`'s horizons by venturing into novel optimization contexts, diversifying the surrogate model repertoire, and probing its efficacy in multi-objective optimization landscapes.

Key areas for future enhancement include the adaptation of the `HomOpt` framework to embrace a wider spectrum of loss functions and the refinement of surrogate model selection processes. Emphasizing mathematical strategies to bolster the framework's scalability and precision, especially within complex, high-dimensional domains, will be pivotal in broadening `HomOpt`'s applicability and impact (Boyd and Vandenberghe, 2004). Moreover, while `HomOpt` navigates the nuances of various loss functions, its flexibility regarding hyperparameter space—unconstrained by data type or dimensionality—further accentuates its utility and adaptability to diverse machine learning tasks.

`HomOpt` offers a promising pathway to refining the efficiency and efficacy of model development across an expansive range of applications. As we continue to push the boundaries of what is possible with HPO, `HomOpt` serves as a catalyst for future innovation, to drive the development of optimization solutions that are both more efficient and universally applicable.

Acknowledgements

This work was funded by DEVCOM Army Research Laboratory under cooperative agreement, W911NF-20-2-0218.

References

Takuya Akiba, Shotaro Sano, Toshihiko Yanase, Takeru Ohta, and Masanori Koyama. Optuna: A next-generation hyperparameter optimization framework. In *Proceedings of the 25th ACM SIGKDD international conference on knowledge discovery & data mining*, pages 2623–2631, 2019.

Vítor Albiero, Kai Zhang, and Kevin W Bowyer. How does gender balance in training data affect face recognition accuracy? In *2020 ieee international joint conference on biometrics (ijcb)*, pages 1–10. IEEE, 2020.

Eugene L. Allgower and Kurt Georg. *Numerical continuation methods*, volume 13 of *Springer Series in Computational Mathematics*. Springer-Verlag, Berlin, 1990. ISBN 3-540-12760-7. doi: 10.1007/978-3-642-61257-2. URL https://doi.org/10.1007/978-3-642-61257-2. An introduction.

Aravind Baskar, Mark Plecnik, and Jonathan D. Hauenstein. Computing saddle graphs via homotopy continuation for the approximate synthesis of mechanisms. *Mechanism and Machine Theory*, 176:104932, 2022.

Daniel J Bates, Andrew J Sommese, Jonathan D Hauenstein, and Charles W Wampler. *Numerically solving polynomial systems with Bertini*. SIAM, 2013.

Yoshua Bengio. Gradient-Based Optimization of Hyperparameters. *Neural Computation*, 12(8):1889–1900, 08 2000. ISSN 0899-7667. doi: 10.1162/089976600300015187. URL https://doi.org/10.1162/089976600300015187.

Yoshua Bengio, Patrice Simard, and Paolo Frasconi. Learning long-term dependencies with gradient descent is difficult. *IEEE Transactions on Neural Networks*, 5(2):157–166, 1994. doi: 10.1109/72.279181.

James Bergstra and Yoshua Bengio. Random search for hyper-parameter optimization. *Journal of Machine Learning Research*, 13(10):281–305, 2012a. URL http://jmlr.org/papers/v13/bergstra12a.html.

James Bergstra and Yoshua Bengio. Random search for hyper-parameter optimization. *Journal of Machine Learning Research*, 13(Feb):281–305, 2012b.

James Bergstra, Rémi Bardenet, Yoshua Bengio, and Balázs Kégl. Algorithms for hyper-parameter optimization. In J. Shawe-Taylor, R. Zemel, P. Bartlett, F. Pereira, and K. Q. Weinberger, editors, *Advances in Neural Information Processing Systems*, volume 24. Curran Associates, Inc., 2011a. URL https://proceedings.neurips.cc/paper/2011/file/86e8f7ab32cfd12577bc2619bc635690-Paper.pdf.

James Bergstra, Rémi Bardenet, Yoshua Bengio, and Balázs Kégl. Algorithms for hyper-parameter optimization. *Advances in neural information processing systems*, 24, 2011b.

James Bergstra, Brent Komer, Chris Eliasmith, Dan Yamins, and David D Cox. Hyperopt: a python library for model selection and hyperparameter optimization. *Computational Science & Discovery*, 8(1):014008, jul 2015. doi: 10.1088/1749-4699/8/1/014008. URL https://doi.org/10.1088/1749-4699/8/1/014008.

Bruno Betrò. Bayesian methods in global optimization. *Operations Research '91*, page 16–18, 1992. doi: 10.1007/978-3-642-48417-9_6.

Atharv Bhosekar and Marianthi Ierapetritou. Advances in surrogate based modeling, feasibility analysis, and optimization: A review. *Computers & Chemical Engineering*, 108:250–267, 2018.

D.W. Boeringer and D.H. Werner. Efficiency-constrained particle swarm optimization of a modified bernstein polynomial for conformal array excitation amplitude synthesis. *IEEE Transactions on Antennas and Propagation*, 53(8):2662–2673, 2005. doi: 10.1109/TAP.2005.851783.

Stephen P Boyd and Lieven Vandenberghe. *Convex optimization*. Cambridge university press, 2004.

Leo Breiman. Random forests. *Machine learning*, 45:5–32, 2001.

Qipin Chen and Wenrui Hao. A homotopy training algorithm for fully connected neural networks. *Proceedings of the Royal Society A: Mathematical, Physical and Engineering Sciences*, 475(2231):20190662, 2019.

J. Chow, L. Udpa, and S.S. Udpa. Homotopy continuation methods for neural networks. In *1991., IEEE International Sympoisum on Circuits and Systems*, pages 2483–2486 vol.5, 1991. doi: 10.1109/ISCAS.1991.176030.

Jiankang Deng, Jia Guo, Jing Yang, Niannan Xue, Irene Kotsia, and Stefanos Zafeiriou. Arcface: Additive angular margin loss for deep face recognition. *IEEE Trans. Pattern Anal. Mach. Intell.*, 44(10):5962–5979, 2022. doi: 10.1109/TPAMI.2021.3087709. URL https://doi.org/10.1109/TPAMI.2021.3087709.

Li Deng. The mnist database of handwritten digit images for machine learning research [best of the web]. *IEEE signal processing magazine*, 29(6):141–142, 2012.

Xuanyi Dong and Yi Yang. Nas-bench-201: Extending the scope of reproducible neural architecture search. In *8th International Conference on Learning Representations, ICLR 2020, Addis Ababa, Ethiopia, April 26-30, 2020*. OpenReview.net, 2020. URL https://openreview.net/forum?id=HJxyZkBKDr.

Anna Veronika Dorogush, Vasily Ershov, and Andrey Gulin. CatBoost: gradient boosting with categorical features support. In *Workshop on ML Systems at NIPS 2017*, 2017.

Kai-Bo Duan and S. Sathiya Keerthi. Which is the best multiclass svm method? an empirical study. In *Proceedings of the 6th International Conference on Multiple Classifier Systems*, MCS'05, page 278–285, Berlin, Heidelberg, 2005. Springer-Verlag. ISBN 3540263063. doi: 10.1007/11494683_28. URL https://doi.org/10.1007/11494683_28.

Katharina Eggensperger, Frank Hutter, Holger H Hoos, and Kevin Leyton-Brown. Surrogate benchmarks for hyperparameter optimization. In *MetaSel@ ECAI*, pages 24–31, 2014.

Katharina Eggensperger, Philipp Müller, Neeratyoy Mallik, Matthias Feurer, René Sass, Aaron Klein, Noor H. Awad, Marius Lindauer, and Frank Hutter. HPOBench: A collection of reproducible multi-fidelity benchmark problems for HPO. In Joaquin Vanschoren and Sai-Kit Yeung, editors, *Proceedings of the Neural Information Processing Systems Track on Datasets and Benchmarks 1, NeurIPS Datasets and Benchmarks 2021, December 2021, virtual*, 2021. URL https://datasets-benchmarks-proceedings.neurips.cc/paper/2021/hash/93db85ed909c13838ff95ccfa94cebd9-Abstract-round2.html.

Stefan Falkner, Aaron Klein, and Frank Hutter. Bohb: Robust and efficient hyperparameter optimization at scale. In *International conference on machine learning*, pages 1437–1446. PMLR, 2018.

Florian Felten, Daniel Gareev, El-Ghazali Talbi, and Grégoire Danoy. Hyperparameter optimization for multi-objective reinforcement learning. *arXiv preprint arXiv:2310.16487*, 2023.

Alexander Forrester, Andras Sobester, and Andy Keane. *Engineering design via surrogate modelling: a practical guide*. John Wiley & Sons, 2008.

Alexander IJ Forrester and Andy J Keane. Recent advances in surrogate-based optimization. *Progress in aerospace sciences*, 45(1-3):50–79, 2009.

Jerome H Friedman. Greedy function approximation: a gradient boosting machine. *Annals of statistics*, pages 1189–1232, 2001.

Zoubin Ghahramani. Learning dynamic bayesian networks. *Adaptive Processing of Sequences and Data Structures: International Summer School on Neural Networks "ER Caianiello" Vietri sul Mare, Salerno, Italy September 6–13, 1997 Tutorial Lectures*, pages 168–197, 2006.

Daniel Golovin, Benjamin Solnik, Subhodeep Moitra, Greg Kochanski, John Karro, and David Sculley. Google vizier: A service for black-box optimization. In *Proceedings of the 23rd ACM SIGKDD international conference on knowledge discovery and data mining*, pages 1487–1495, 2017.

Robert B. Gramacy and Herbert K. H. Lee. Cases for the nugget in modeling computer experiments. *Stat. Comput.*, 22(3):713–722, 2012.

Zachary A Griffin and Jonathan D Hauenstein. Real solutions to systems of polynomial equations and parameter continuation. *Advances in Geometry*, 15(2):173–187, 2015.

Yandong Guo, Lei Zhang, Yuxiao Hu, Xiaodong He, and Jianfeng Gao. Ms-celeb-1m: A dataset and benchmark for large-scale face recognition. In *European conference on computer vision*, pages 87–102. Springer, 2016.

Trevor J Hastie and Rob J Tibshirani. Generalized additive models, volume 43 of. *Monographs on statistics and applied probability*, 15, 1990.

Gary B. Huang, Manu Ramesh, Tamara Berg, and Erik Learned-Miller. Labeled faces in the wild: A database for studying face recognition in unconstrained environments. Technical Report 07-49, University of Massachusetts, Amherst, October 2007.

Frank Hutter, Lars Kotthoff, and Joaquin Vanschoren. *Automated machine learning: methods, systems, challenges*. Springer Nature, 2019.

Ilija Ilievski, Taimoor Akhtar, Jiashi Feng, and Christine Shoemaker. Efficient hyperparameter optimization for deep learning algorithms using deterministic rbf surrogates. In *Proceedings of the AAAI Conference on Artificial Intelligence*, volume 31, 2017.

Hidenori Iwakiri, Yuhang Wang, Shinji Ito, and Akiko Takeda. Single loop gaussian homotopy method for non-convex optimization. *Advances in Neural Information Processing Systems*, 35:7065–7076, 2022.

Kirthevasan Kandasamy, Akshay Krishnamurthy, Jeff Schneider, and Barnabás Póczos. Parallelised bayesian optimisation via thompson sampling. In *International Conference on Artificial Intelligence and Statistics*, pages 133–142. PMLR, 2018.

James Kennedy and Russell Eberhart. Particle swarm optimization. In *Proceedings of ICNN'95-international conference on neural networks*, volume 4, pages 1942–1948. IEEE, 1995.

J. Kinnison, N. Kremer-Herman, D. Thain, and W. Scheirer. Shadho: Massively scalable hardware-aware distributed hyperparameter optimization. In *2018 IEEE Winter Conference on Applications of Computer Vision (WACV)*, pages 738–747, 2018. doi: 10.1109/WACV.2018.00086.

Lisha Li, Kevin Jamieson, Giulia DeSalvo, Afshin Rostamizadeh, and Ameet Talwalkar. Hyperband: A novel bandit-based approach to hyperparameter optimization. *The Journal of Machine Learning Research*, 18 (1):6765–6816, 2017.

Andy Liaw, Matthew Wiener, et al. Classification and regression by randomforest. *R news*, 2(3):18–22, 2002.

Marius Lindauer, Katharina Eggensperger, Matthias Feurer, Stefan Falkner, André Biedenkapp, and Frank Hutter. Smac v3: Algorithm configuration in python. `https://github.com/automl/SMAC3`, 2017.

Sulin Liu, Qing Feng, David Eriksson, Benjamin Letham, and Eytan Bakshy. Sparse bayesian optimization. In *International Conference on Artificial Intelligence and Statistics*, pages 3754–3774. PMLR, 2023.

Ilya Loshchilov and Frank Hutter. CMA-ES for hyperparameter optimization of deep neural networks. In *International Conference on Learning Representations (ICLR 2016). Workshop Track.*, pages 1–4, 2016.

Dougal Maclaurin, David Duvenaud, and Ryan P. Adams. Gradient-based hyperparameter optimization through reversible learning. In Francis R. Bach and David M. Blei, editors, *Proceedings of the 32nd International Conference on Machine Learning, ICML 2015, Lille, France, 6-11 July 2015*, volume 37 of *JMLR Workshop and Conference Proceedings*, pages 2113–2122. JMLR.org, 2015. URL http://proceedings.mlr.press/v37/maclaurin15.html.

Mark McLeod, Stephen J. Roberts, and Michael A. Osborne. Optimization, fast and slow: Optimally switching between local and bayesian optimization. In Jennifer G. Dy and Andreas Krause, editors, *Proceedings of the 35th International Conference on Machine Learning, ICML 2018, Stockholmsmässan, Stockholm, Sweden, July 10-15, 2018*, volume 80 of *Proceedings of Machine Learning Research*, pages 3440–3449. PMLR, 2018. URL http://proceedings.mlr.press/v80/mcleod18a.html.

Dhagash Mehta, Tianran Chen, Tingting Tang, and Jonathan D. Hauenstein. The loss surface of deep linear networks viewed through the algebraic geometry lens. *IEEE Transactions on Pattern Analysis and Machine Intelligence*, 44(9):5664–5680, 2022.

J. A. Nelder and R. Mead. A Simplex Method for Function Minimization. *The Computer Journal*, 7(4): 308–313, 01 1965. ISSN 0010-4620. doi: 10.1093/comjnl/7.4.308. URL https://doi.org/10.1093/comjnl/7.4.308.

Robert Nisbet. *Handbook of statistical analysis and data mining applications*. Academic Press, an imprint of Elsevier, London, United Kingdom, second edition edition, 2018.

Sinno Jialin Pan and Qiang Yang. A survey on transfer learning. *IEEE Transactions on knowledge and data engineering*, 22(10):1345–1359, 2009.

Harsh Nilesh Pathak. *Parameter Continuation with Secant Approximation for Deep Neural Networks*. PhD thesis, Worcester Polytechnic Institute, 2018.

Liudmila Prokhorenkova, Gleb Gusev, Aleksandr Vorobev, Anna Veronika Dorogush, and Andrey Gulin. Catboost: unbiased boosting with categorical features. *Advances in neural information processing systems*, 31, 2018.

Carl Edward Rasmussen, Christopher KI Williams, et al. *Gaussian processes for machine learning*, volume 1. Springer, 2006.

Werner C. Rheinboldt. Numerical analysis of continuation methods for nonlinear structural problems. *Computers & Structures*, 13(1):103–113, 1981. ISSN 0045-7949. doi: https://doi.org/10.1016/0045-7949(81)90114-0. URL https://www.sciencedirect.com/science/article/pii/0045794981901140.

Luis Miguel Rios and Nikolaos V Sahinidis. Derivative-free optimization: a review of algorithms and comparison of software implementations. *Journal of Global Optimization*, 56:1247–1293, 2013.

Jairo Rojas-Delgado, JA Jiménez, Rafael Bello, and José Antonio Lozano. Hyper-parameter optimization using continuation algorithms. In *Metaheuristics International Conference*, pages 365–377. Springer, 2022.

Ethan M Rudd, Lalit P Jain, Walter J Scheirer, and Terrance E Boult. The extreme value machine. *IEEE transactions on pattern analysis and machine intelligence*, 40(3):762–768, 2017.

Walter J. Scheirer, Anderson Rocha, Archana Sapkota, and Terrance E. Boult. Towards open set recognition. *IEEE Transactions on Pattern Analysis and Machine Intelligence (T-PAMI)*, 35:1757–1772, July 2012.

Daniel Servén, Charlie Brummitt, Hassan Abedi, and hlink. dswah/pygam: v0.8.0. Zenodo, 2018.

Burr Settles. Active learning literature survey. University of Wisconsin-Madison Department of Computer Sciences, 2009.

Andrew J. Sommese and Charles W. Wampler, II. *The numerical solution of systems of polynomials arising in engineering and science*. World Scientific Publishing Co. Pte. Ltd., Hackensack, NJ, 2005.

Rainer Storn and Kenneth Price. Differential evolution–a simple and efficient heuristic for global optimization over continuous spaces. *Journal of global optimization*, 11:341–359, 1997.

Sonja Surjanovic and Derek Bingham. Virtual library of simulation experiments: Griewank function, 2013. URL `https://www.sfu.ca/~ssurjano/griewank.html`.

Richard S Sutton and Andrew G Barto. *Reinforcement learning: An introduction*. MIT press, 2018.

Shinya Suzumura, Kohei Ogawa, Masashi Sugiyama, Masayuki Karasuyama, and Ichiro Takeuchi. Homotopy continuation approaches for robust sv classification and regression. *Machine Learning*, 106:1009–1038, 2017.

Robert Tibshirani and Trevor Hastie. Local likelihood estimation. *Journal of the American Statistical Association*, 82(398):559–567, 1987.

Joaquin Vanschoren, Jan N Van Rijn, Bernd Bischl, and Luis Torgo. Openml: networked science in machine learning. *ACM SIGKDD Explorations Newsletter*, 15(2):49–60, 2014.

Layne T Watson, Maria Sosonkina, Robert C Melville, Alexander P Morgan, and Homer F Walker. Algorithm 777: Hompack90: A suite of fortran 90 codes for globally convergent homotopy algorithms. *ACM Transactions on Mathematical Software (TOMS)*, 23(4):514–549, 1997.

Jia Wu, Xiu-Yun Chen, Hao Zhang, Li-Dong Xiong, Hang Lei, and Si-Hao Deng. Hyperparameter optimization for machine learning models based on bayesian optimizationb. *Journal of Electronic Science and Technology*, 17(1):26–40, 2019. ISSN 1674-862X. doi: https://doi.org/10.11989/JEST.1674-862X.80904120. URL `https://www.sciencedirect.com/science/article/pii/S1674862X19300047`.

Weicheng Xie, Wenting Chen, Linlin Shen, Jinming Duan, and Meng Yang. Surrogate network-based sparseness hyper-parameter optimization for deep expression recognition. *Pattern Recognition*, 111: 107701, 2021. ISSN 0031-3203. doi: https://doi.org/10.1016/j.patcog.2020.107701. URL `https://www.sciencedirect.com/science/article/pii/S0031320320305045`.

Kiyotaka Yamamura, Tooru Sekiguchi, and Yasuaki Inoue. A fixed-point homotopy method for solving modified nodal equations. *IEEE Transactions on Circuits and Systems I: Fundamental Theory and Applications*, 46(6):654–665, 1999.

Yudong Zhang, Shuihua Wang, Genlin Ji, et al. A comprehensive survey on particle swarm optimization algorithm and its applications. *Mathematical problems in engineering*, 2015, 2015.

Appendix A. Meta-Parameter Analysis

A.1 Meta-Parameter Sensitivity Analysis on XGBoost Benchmark

Since `HomOpt` demonstrated minimal improvement on the XGBoost benchmark, we performed an additional study on one of the datasets to illustrate the sensitivity of parameters within `HomOpt` on the performance of the optimization. On dataset credit-g, we run `HomOpt` for each of the base sampling methods (Bayes, Random, SMAC, TPE), with the method parameters and domains indicated in Table 8. This search was done over 100 iterations for a single seed for each combination of method parameters. The studies visualized in the contour plot (Figure 13) with SMAC samples, revealed that the performance of the optimization using `HomOpt` is sensitive to the choice of corresponding method parameters and domains. In our experiments our default method parameters use a k of 0.5, five iterations to compute the homotopy, a jitter strength of 0.005 and 20 warm up samples. The contour plot demonstrates how changes in these method parameter values can affect the optimization performance, where certain regions have higher performance (indicated by a lower loss value which are the blue regions). In this case, a higher k value of 0.6 and more warm samples (30+) resulted in higher performance for this dataset.

Variable	Description	Domain
$\mathcal{D}$	Local perturbation factor	[5, 5e-1, 5e-2, 5e-3, 5e-4, 5e-5]
$\mathcal{W}$	Number of warm-up samples	[10, 30, 50, 70, 90]
$\mathcal{N}$	Number of minimization steps to compute homotopy	[3, 6, 9]
k	Fraction of completed trials to train the GAMs	[0.2, 0.4, 0.6, 0.8, 1]

Table 8: `HomOpt` parameters and domain spaces for ablation study on XGBoost benchmark.

A pivotal direction for future work involves developing more sophisticated techniques for intelligently determining optimal method parameters, akin to how BOHB automates the configuration of its optimization process. This entails leveraging machine learning models or meta-learning approaches to predict optimal parameter settings based on dataset characteristics or previous optimization outcomes. Such advancements could include:

- **Automated Parameter Tuning**: Implement algorithms to dynamically refine `HomOpt`'s parameters, adjusting based on real-time optimization metrics.
- **Meta-Learning for Parameter Selection**: Utilize meta-learning to predict optimal parameter settings from historical optimization data, reducing the need for manual tuning.
- **Adaptive Sampling Techniques**: Integrate strategies that modulate exploration and exploitation balance according to the optimization landscape's observed sensitivity.
- **Performance Prediction Models**: Develop models to foresee the impact of parameter adjustments on optimization outcomes, guiding initial `HomOpt` configurations towards efficiency.

These initiatives aim to bolster `HomOpt`'s performance and versatility, ensuring its broader applicability and reduced dependency on manual parameter tuning.

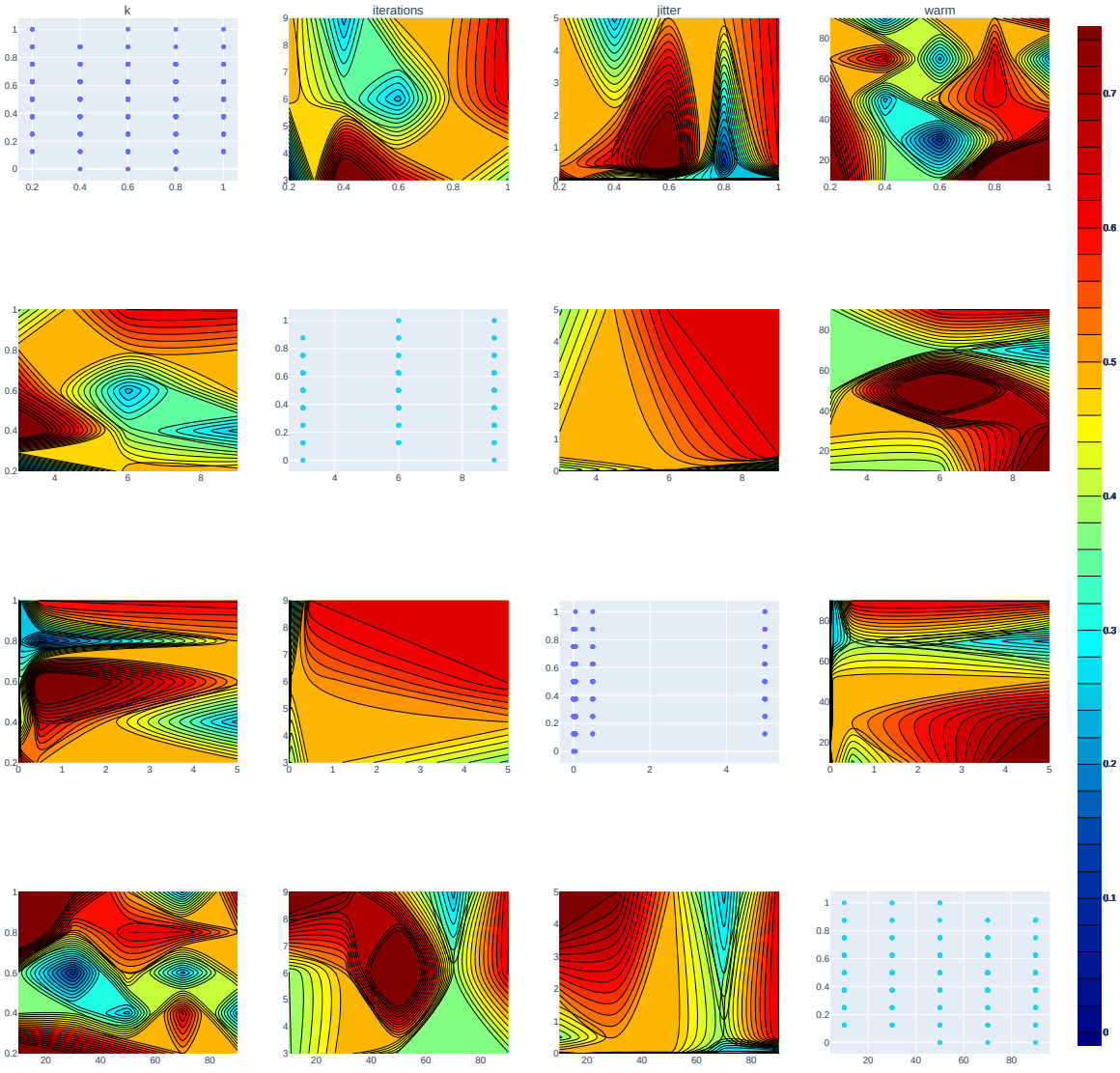

Figure 13: Contour plots visualizing the interactions between pairs of method parameters with SMAC samples on XGBoost sensitivity study. In this plot k represents the proportion of trial data used to train one of the GAMs, $iterations$ are the number of minimizations to compute the homotopy, $jitter$ refers to the distance threshold as the local perturbation search around the observed minimum and $warm$ represents the number of samples used for the surrogate approximation. Changes in the method parameter values can affect the optimization performance, where certain regions have higher performance (indicated by a lower loss value which are the blue regions)

Appendix B. Enhancing Interpretability in Hyperparameter Optimization with GAMs

GAMs offer greater interpretability over more complex models, which can be for hyperparameter optimization. This study focused on optimizing the Branin function, a commonly used test function in optimization studies, defined by:

$$f(x_1, x_2) = a(x_2 - bx_1^2 + cx_1 - r)^2 + s(1-t)\cos(x_1) + s,$$

where $a = 1$, $b = \frac{5.1}{4\pi^2}$, $c = \frac{5}{\pi}$, $r = 6$, $s = 10$, and $t = \frac{1}{8\pi}$. The hyperparameters x_1 and x_2 ranged from $[-5, 10]$ and $[0, 15]$, respectively. The optimization was performed employing `HomOpt` with random sampling method across 100 evaluations.

The analysis utilized partial dependence plots to illustrate how variations in each hyperparameter (x_1 and x_2) independently influence the output of the Branin function. These visualizations revealed critical sensitivities; particularly, x_1 displayed non-linear effects with distinct peaks and troughs indicating regions of high sensitivity, while x_2 showed a more linear relationship, suggesting straightforward adjustments can effectively optimize this parameter. The optimization landscape, visualized in the contour plot, highlighted the distribution of tested hyperparameter combinations and their corresponding outputs, revealing both the global search behavior and focal points of optimization.

Figure 14: Visualization of hyperparameter effects and optimization landscape using Generalized Additive Models (GAMs). The first panel displays the partial dependence of the Branin function on hyperparameter x_1 with a 95% confidence interval, highlighting the non-linear impact of x_1 on the model output. The second panel shows the partial dependence for hyperparameter x_2 , illustrating its predominantly increasing influence on the Branin function, defined within a 95% confidence interval. The final panel depicts the optimization landscape over the x_1 and x_2 space, with white dots representing tested parameter combinations and the red dot marking the optimal setting. This panel visually corroborates the areas of interest identified in the partial dependence plots and demonstrates the coverage of the search space by the optimization process.

By leveraging partial dependence plots, GAMs provide a clear visualization of how variations in each hyperparameter affect model performance, revealing critical non-linear relationships and sensitivities. Such insights allow practitioners to prioritize which hyperparameters to tune, adjust their ranges effectively to avoid overfitting and underfitting, and implement adaptive sampling strategies to focus computational resources on promising areas of the hyperparameter space. This not

only optimizes the efficiency of the search process but also supports dynamic adjustments based on emerging data insights.

Appendix C. Extended EVM Results

Here we include additional results from the experiments. In the EVM experiments, we report the corresponding Normalized Mutual Information (NMI) score for each experiment which measures the similarity between the predicted label and the true class label as well.

$$\text{NMI}(C,T) = \frac{2 \times I(C,T)}{H(C) + H(T)} \tag{10}$$

$$\text{H}(C) = -\sum_{c} p(c) \log_2 p(c) \tag{11}$$

$$\text{H}(T) = -\sum_{t} p(t) \log_2 p(t) \tag{12}$$

Table 9 reported the validation and testing score for MNIST data set experiments for open set recognition. In general, we can see the results for `HomOpt` are improved against all the base strategies random, TPE, Bayes, and SMAC. We can see consistent results (see Table 10) in the LFW experiment improves among all the base methods. It is noticeable that the highest validation and testing scores for MNIST data set achieves from the `HomOpt` with random seeds used for warm-up, while LFW data set achieves the highest scores from the `HomOpt` with SMAC seeds used for warm-up trials.

Method	Validation F1	Validation Accuracy	Validation NMI	Testing F1	Testing Accuracy	Testing NMI
Random	0.8982 ± 0.006	0.8958 ± 0.007	0.7547 ± 0.014	0.8988 ± 0.005	0.8969 ± 0.007	0.7579 ± 0.013
PSHHO+Random	$\mathbf{0.9160 \pm 0.003}$	$\mathbf{0.9127 \pm 0.004}$	$\mathbf{0.7889 \pm 0.008}$	$\mathbf{0.9039 \pm 0.006}$	$\mathbf{0.9022 \pm 0.007}$	$\mathbf{0.7657 \pm 0.012}$
TPE	0.8889 ± 0.011	0.8859 ± 0.011	0.7431 ± 0.022	0.8788 ± 0.004	0.8766 ± 0.004	0.7287 ± 0.009
PSHHO+TPE	0.9140 ± 0.003	0.9106 ± 0.004	0.7838 ± 0.005	0.8982 ± 0.007	0.8964 ± 0.006	0.7579 ± 0.012
Bayes	0.8771 ± 0.008	0.8749 ± 0.006	0.7200 ± 0.015	0.8669 ± 0.010	0.8655 ± 0.008	0.7054 ± 0.018
PSHHO+Bayes	0.9132 ± 0.002	0.9092 ± 0.003	0.7793 ± 0.003	0.8995 ± 0.003	0.8981 ± 0.004	0.7583 ± 0.004
SMAC	0.9034 ± 0.005	0.9001 ± 0.006	0.7650 ± 0.013	0.8924 ± 0.006	0.8907 ± 0.007	0.7468 ± 0.013
PSHHO+SMAC	0.9110 ± 0.006	0.9081 ± 0.005	0.7797 ± 0.009	0.8992 ± 0.004	0.8976 ± 0.005	0.7599 ± 0.008

Table 9: Average validation/testing score comparison for each base method and corresponding homotopy approach across 5 separate seeds for the EVM experiments with MNIST dataset.

Method	Validation F1	Validation Accuracy	Validation NMI	Testing F1	Testing Accuracy	Testing NMI
Random	0.8556 ± 0.009	0.9659 ± 0.004	0.8254 ± 0.019	0.8191 ± 0.058	0.9596 ± 0.028	0.7927 ± 0.011
PSHHO+Random	0.8654 ± 0.004	0.9673 ± 0.001	0.8309 ± 0.009	$\mathbf{0.8248 \pm 0.015}$	0.9610 ± 0.002	0.7981 ± 0.011
TPE	0.8400 ± 0.018	0.9618 ± 0.006	0.8060 ± 0.026	0.7992 ± 0.026	0.9554 ± 0.005	0.7729 ± 0.024
PSHHO+TPE	0.8563 ± 0.016	0.9632 ± 0.007	0.8140 ± 0.030	0.8175 ± 0.014	0.9571 ± 0.005	0.7844 ± 0.023
Bayes	0.8426 ± 0.007	0.9617 ± 0.002	0.8049 ± 0.010	0.7919 ± 0.013	0.9542 ± 0.003	0.7657 ± 0.014
PSHHO+Bayes	0.8622 ± 0.008	0.9671 ± 0.003	0.8288 ± 0.016	0.8161 ± 0.015	0.9589 ± 0.003	0.78855 ± 0.015
SMAC	0.8510 ± 0.004	0.9657 ± 0.003	0.8241 ± 0.014	0.8218 ± 0.016	0.9602 ± 0.003	0.7951 ± 0.003
PSHHO+SMAC	$\mathbf{0.8698 \pm 0.005}$	$\mathbf{0.9699 \pm 0.001}$	$\mathbf{0.8433 \pm 0.007}$	0.8231 ± 0.010	$\mathbf{0.9613 \pm 0.002}$	$\mathbf{0.8001 \pm 0.009}$

Table 10: Average validation/testing scores comparison for each base method and corresponding homotopy approach across 5 separate seeds for the EVM experiment with LFW dataset.

C.1 Extended HPOBench Results

In this section, we present the additional results for the HPOBench experiments, specifically focusing on the validation and test scores. The validation and test scores showcase the average percent improvement and standard error achieved over 5 trials for each dataset experiment within the benchmark.

C.1.1 VALIDATIONS SCORES

Table 11: Average percent improvement and standard error for the best observed loss over five trials of `HomOpt` *over the base methodology for each dataset and method in the SVM Benchmark. Bold values indicate where* `HomOpt` *outperforms the base methodology.*

Dataset	Method			
	bayes	**random**	**smac**	**tpe**
10101	**5.22** ± 1.63	**4.35** ± 2.38	**8.33** ± 1.32	**5.22** ± 2.54
12	**1.05** ± 0.43	**1.05** ± 0.43	**1.63** ± 0.94	**1.40** ± 0.47
146818	**29.52** ± 17.26	**55.24** ± 12.74	**52.38** ± 12.78	-40.00 ± 44.97
146821	-3.24 ± 1.01	**54.29** ± 26.30	**57.84** ± 25.82	**16.76** ± 20.82
146822	**67.24** ± 1.09	**40.65** ± 2.62	-8.24 ± 5.46	**47.78** ± 1.36
168911	**21.87** ± 5.96	-40.45 ± 11.20	**3.23** ± 10.08	**15.11** ± 8.84
168912	**38.63** ± 16.36	**45.12** ± 15.89	**47.43** ± 14.96	**27.10** ± 16.45
3	**56.34** ± 25.81	**9.68** ± 85.50	**98.47** ± 0.68	-587.50 ± 416.03
31	-10.00 ± 5.39	-10.00 ± 5.39	-10.00 ± 5.39	-10.00 ± 5.39
3917	**2.50** ± 1.67	**2.50** ± 1.67	**2.50** ± 1.67	**2.50** ± 1.67
53	**41.54** ± 17.77	**28.67** ± 22.20	**0.00** ± 28.69	-33.75 ± 42.09
9952	-14.86 ± 17.23	-1.59 ± 4.29	-1.72 ± 3.53	-1.64 ± 3.77
9981	-2.75 ± 1.27	-2.00 ± 0.94	-2.75 ± 1.27	-3.00 ± 1.40

Table 12: Average percent improvement and standard error for the best observed loss over five trials of `HomOpt` *over the base methodology for each dataset and method in the Random Forest benchmark. Bold values indicate where* `HomOpt` *outperforms the base methodology.*

Dataset	Method			
	bayes	**random**	**smac**	**tpe**
10101	**35.12** ± 8.78	**28.24** ± 3.55	**17.14** ± 1.75	-5.00 ± 9.26
12	**60.00** ± 10.95	**35.00** ± 6.12	**48.00** ± 8.00	-120.00 ± 37.42
146818	**61.82** ± 16.61	**63.08** ± 4.49	**42.22** ± 6.48	**16.67** ± 11.79
146821	**93.04** ± 1.06	**80.00** ± 6.48	**0.00** ± 15.81	-40.00 ± 24.49
146822	**69.70** ± 3.95	**38.95** ± 11.36	**24.62** ± 7.46	**3.64** ± 16.91
167119	**46.36** ± 0.15	**34.72** ± 0.27	**3.99** ± 1.19	**0.59** ± 0.30
168911	**54.29** ± 2.81	**22.32** ± 8.68	**13.21** ± 2.00	-0.00 ± 2.83
168912	**73.75** ± 2.00	**40.00** ± 1.17	**28.00** ± 3.58	**14.74** ± 3.07
31	**45.71** ± 13.24	**38.00** ± 6.80	**15.24** ± 5.51	-41.18 ± 42.78
3917	**61.61** ± 2.00	**49.33** ± 1.91	**29.41** ± 2.08	**24.83** ± 2.76
53	**64.44** ± 1.04	**42.50** ± 3.33	-9.09 ± 7.61	**1.67** ± 3.12
9952	**63.68** ± 1.95	**29.18** ± 2.22	**25.26** ± 2.58	**1.43** ± 2.45
9981	**81.67** ± 3.12	**40.00** ± 6.12	**30.00** ± 12.25	**60.00** ± 6.32

Table 13: Average percent improvement and standard error for the best observed loss over five trials of `HomOpt` *over the base methodology for each dataset and method in the Logistic Regression Benchmark. Bold values indicate where* `HomOpt` *outperforms the base methodology.*

Dataset	Method			
	bayes	**random**	**smac**	**tpe**
10101	**9.41** ± 1.44	**6.40** ± 1.60	**4.08** ± 1.12	**7.60** ± 1.47
12	**78.79** ± 18.21	**90.00** ± 4.84	**75.00** ± 0.00	**35.79** ± 37.19
146212	**39.34** ± 15.76	**46.21** ± 7.74	**37.63** ± 5.04	**44.88** ± 7.69
146606	**17.02** ± 2.16	**4.57** ± 1.40	**6.01** ± 0.04	**5.94** ± 2.32
146818	**16.88** ± 3.37	**19.33** ± 0.67	**12.14** ± 1.43	**20.67** ± 0.67
146821	**29.49** ± 1.67	**27.44** ± 3.82	**16.77** ± 2.14	-3.46 ± 3.24
146822	**7.93** ± 10.59	**1.91** ± 7.37	**9.21** ± 2.23	**25.00** ± 3.17
14965	**4.33** ± 2.44	**4.82** ± 1.30	**2.91** ± 2.01	**3.03** ± 2.28
167119	**2.96** ± 0.17	**1.04** ± 0.20	**0.67** ± 0.02	**2.73** ± 0.37
167120	-0.05 ± 0.13	**0.38** ± 0.21	-0.45 ± 0.21	**0.66** ± 0.39
168911	**19.55** ± 1.75	**3.85** ± 2.27	-1.62 ± 1.77	-0.44 ± 2.24
168912	**25.96** ± 6.75	**4.63** ± 4.89	**8.83** ± 0.57	**9.50** ± 8.18
3	**69.43** ± 10.67	**67.37** ± 0.49	**19.37** ± 2.69	**49.68** ± 17.90
31	**17.25** ± 1.87	**10.56** ± 2.73	**8.29** ± 2.98	**9.46** ± 2.93
3917	**0.92** ± 1.23	-0.23 ± 1.24	**1.36** ± 0.23	-1.40 ± 0.23
53	**17.78** ± 14.46	**18.06** ± 3.86	**20.00** ± 1.81	**31.85** ± 13.24
7592	**7.64** ± 2.28	**3.89** ± 3.50	**4.28** ± 0.08	-1.36 ± 3.21
9952	**2.13** ± 1.08	**2.98** ± 0.61	-0.35 ± 0.63	-3.18 ± 0.31
9977	**24.91** ± 9.65	**20.36** ± 8.15	**25.20** ± 0.29	**7.44** ± 11.08
9981	**83.08** ± 4.49	**30.00** ± 9.35	**55.00** ± 14.58	**65.71** ± 11.61

Table 14: Average percent improvement and standard error for the best observed loss over five trials of `HomOpt` *over the base methodology for each dataset and method in the MLP Benchmark. Bold values indicate where* `HomOpt` *outperforms the base methodology.*

Dataset	Method			
	bayes	**random**	**smac**	**tpe**
10101	**3.72** ± 0.57	**0.98** ± 1.65	**7.14** ± 3.69	**3.90** ± 1.65
146818	**57.50** ± 3.64	**17.50** ± 3.06	-32.00 ± 8.00	**20.00** ± 7.28
146822	**59.22** ± 0.73	**43.59** ± 4.51	**30.67** ± 0.67	**50.73** ± 1.42
31	**40.00** ± 2.07	**35.56** ± 5.05	**25.83** ± 4.04	**4.44** ± 4.44
53	**78.46** ± 5.10	**44.62** ± 2.88	**40.00** ± 2.23	**40.00** ± 8.37

Table 15: Average percent improvement and standard error for the best observed loss over five trials of `HomOpt` *over the base methodology for each dataset and method in the XGBoost Benchmark. Bold values indicate where* `HomOpt` *outperforms the base methodology.*

Dataset	Method			
	bayes	**random**	**smac**	**tpe**
10101	**17.33** $\pm$ 2.21	**13.79** $\pm$ 1.54	-10.91 $\pm$ 1.82	-5.45 $\pm$ 0.91
146822	-11.43 $\pm$ 5.35	-22.86 $\pm$ 3.50	-17.14 $\pm$ 5.35	-5.71 $\pm$ 5.71
168912	-2.67 $\pm$ 6.18	-9.33 $\pm$ 6.53	-11.43 $\pm$ 5.35	**1.25** $\pm$ 5.00
31	-5.00 $\pm$ 4.59	**6.67** $\pm$ 2.08	-7.50 $\pm$ 1.25	**10.00** $\pm$ 2.08
3917	-27.00 $\pm$ 2.00	**9.60** $\pm$ 4.66	-8.18 $\pm$ 4.64	-3.48 $\pm$ 5.74
53	**5.45** $\pm$ 6.17	-8.00 $\pm$ 3.74	-4.00 $\pm$ 8.12	**0.00** $\pm$ 5.48
9952	-1.28 $\pm$ 2.48	**6.27** $\pm$ 1.90	-1.28 $\pm$ 1.28	**0.43** $\pm$ 3.10

C.1.2 TEST SCORES

Table 16: Average percent improvement and standard error for the corresponding test loss (1-accuracy) at best observed loss over five trials of `HomOpt` over the base methodology for each dataset and method in the RandomForestBenchmark. Bold values indicate where `HomOpt` outperforms the base methodology.

method dataset	**bayes**	**random**	**smac**	**tpe**
10101	-11.76 ± 3.22	-2.22 ± 5.98	-13.33 ± 2.22	-9.47 ± 5.10
12	**11.11** ± 6.09	**2.86** ± 5.35	-11.43 ± 5.35	-36.00 ± 9.80
146818	-8.57 ± 5.71	**20.00** ± 8.89	-0.00 ± 10.46	**7.50** ± 9.35
146821	**56.92** ± 5.76	**4.00** ± 16.00	-26.67 ± 26.67	-86.67 ± 34.32
146822	-15.29 ± 4.40	-32.86 ± 8.63	**5.88** ± 6.17	-35.71 ± 3.91
167119	-16.40 ± 1.16	-7.15 ± 0.82	**0.27** ± 0.85	-0.94 ± 0.89
168911	**2.76** ± 2.01	-5.00 ± 1.91	-3.21 ± 1.54	**2.86** ± 1.34
168912	-0.54 ± 3.35	**2.11** ± 3.16	-1.11 ± 4.94	-1.11 ± 1.67
31	**15.17** ± 5.52	**15.20** ± 5.28	**12.80** ± 10.23	**15.56** ± 3.95
3917	**2.76** ± 4.28	**8.97** ± 3.71	**5.33** ± 3.27	-3.08 ± 4.93
53	**10.43** ± 3.53	**8.70** ± 5.99	**11.82** ± 1.82	-6.32 ± 6.09
9952	**22.00** ± 4.25	-6.27 ± 2.93	**3.16** ± 4.35	**16.77** ± 2.42
9981	**23.33** ± 12.47	**3.33** ± 9.72	-120.00 ± 37.42	**4.00** ± 9.80

Table 17: Average percent improvement and standard error for the corresponding test loss (1-accuracy) at best observed loss over five trials of `HomOpt` over the base methodology for each dataset and method in the SVMBenchmark. Bold values indicate where `HomOpt` outperforms the base methodology.

method dataset	**bayes**	**random**	**smac**	**tpe**
10101	-3.75 ± 2.50	-5.00 ± 2.34	**2.35** ± 2.35	-5.00 ± 2.34
12	**0.22** ± 0.14	**0.22** ± 0.14	**4.11** ± 3.84	**1.44** ± 1.31
146818	**32.26** ± 19.75	**62.58** ± 15.72	**64.52** ± 16.42	-105.00 ± 74.96
146821	**0.00** ± 0.00	**27.33** ± 41.12	**59.23** ± 24.18	**18.46** ± 18.46
146822	**57.08** ± 1.06	-5.71 ± 5.91	**17.50** ± 5.17	**53.06** ± 2.41
168911	**33.15** ± 8.37	-71.51 ± 20.25	-9.64 ± 16.05	**25.37** ± 11.27
168912	**36.48** ± 15.05	**35.40** ± 16.11	**37.20** ± 15.49	**23.12** ± 14.28
3	**56.34** ± 23.00	-31.72 ± 99.04	**94.25** ± 0.48	-1224.00 ± 708.84
31	**0.00** ± 0.00	**0.00** ± 0.00	**0.00** ± 0.00	**0.00** ± 0.00
3917	-0.00 ± 0.96	-0.00 ± 0.96	-0.00 ± 0.96	-0.00 ± 0.96
53	**37.46** ± 14.15	-2.86 ± 24.42	-23.33 ± 22.92	-62.22 ± 35.94
9952	-16.94 ± 22.46	-15.25 ± 6.72	**9.41** ± 2.96	**0.60** ± 8.32
9981	-0.65 ± 0.43	-1.09 ± 0.69	-1.54 ± 0.56	-0.65 ± 0.55

Table 18: Average percent improvement and standard error for the corresponding test loss (1-accuracy) at best observed loss over five trials of `HomOpt` *over the base methodology for each dataset and method in the LRBenchmark. Bold values indicate where* `HomOpt` *outperforms the base methodology.*

method dataset	**bayes**	**random**	**smac**	**tpe**
10101	-4.44 ± 1.11	-6.67 ± 2.08	**5.26** ± 2.35	**8.00** ± 2.55
12	**64.71** ± 11.91	**36.00** ± 7.48	**43.33** ± 6.67	**52.50** ± 17.74
146212	**39.01** ± 15.89	**45.74** ± 7.84	**36.41** ± 5.63	**44.18** ± 7.26
146606	**16.73** ± 1.74	**3.42** ± 1.37	**5.84** ± 0.12	**5.89** ± 1.97
146818	-8.57 ± 16.66	**20.00** ± 7.07	**11.11** ± 11.65	-33.33 ± 10.54
146821	**30.34** ± 4.55	**29.66** ± 3.55	**18.46** ± 5.63	-4.55 ± 3.80
146822	**22.45** ± 8.09	-2.86 ± 9.52	-16.30 ± 1.89	**36.73** ± 2.66
14965	**2.85** ± 1.97	-0.99 ± 1.64	**1.65** ± 2.42	**1.03** ± 2.29
167119	**4.02** ± 0.34	-0.25 ± 0.43	**1.17** ± 0.19	**3.58** ± 0.43
167120	**0.30** ± 0.20	**0.96** ± 0.14	**0.58** ± 0.48	**1.16** ± 0.62
168911	**4.51** ± 1.29	-8.57 ± 1.19	-8.20 ± 1.16	-2.46 ± 2.73
168912	**20.79** ± 5.17	**1.11** ± 4.25	**1.13** ± 0.96	**13.82** ± 5.36
3	**67.89** ± 12.47	**57.78** ± 3.23	**33.33** ± 4.22	**46.15** ± 18.84
31	**10.00** ± 6.43	**10.71** ± 7.41	**12.86** ± 4.16	**19.37** ± 4.98
3917	**1.88** ± 2.90	-14.29 ± 2.53	**7.27** ± 0.74	**1.88** ± 2.90
53	**0.87** ± 17.25	**24.17** ± 6.37	**5.56** ± 3.04	**18.26** ± 12.33
7592	**9.55** ± 2.40	**5.15** ± 4.00	**1.66** ± 0.28	-1.59 ± 3.88
9952	**0.32** ± 1.50	-0.16 ± 0.60	-2.58 ± 0.16	-2.15 ± 1.00
9977	**20.85** ± 8.66	**21.50** ± 7.28	**18.12** ± 0.63	**7.77** ± 9.79
9981	-3.33 ± 20.68	-30.00 ± 14.58	**10.00** ± 11.30	**5.71** ± 16.66

Table 19: Average percent improvement and standard error for the corresponding test loss (1-accuracy) at best observed loss over five trials of `HomOpt` *over the base methodology for each dataset and method in the NNBenchmark. Bold values indicate where* `HomOpt` *outperforms the base methodology.*

method dataset	**bayes**	**random**	**smac**	**tpe**
10101	**0.00** ± 1.76	**1.05** ± 1.97	-0.00 ± 2.88	-3.33 ± 2.22
146818	-57.14 ± 10.10	-25.00 ± 11.18	**1.82** ± 6.68	-32.50 ± 9.35
146822	**39.13** ± 4.96	**20.00** ± 11.42	**12.00** ± 4.90	**30.59** ± 6.81
31	**3.85** ± 2.43	**8.46** ± 3.73	-3.48 ± 1.63	**9.23** ± 4.65
53	**21.54** ± 7.46	**21.33** ± 3.27	**20.00** ± 4.71	**1.54** ± 9.23

Table 20: Average percent improvement and standard error for the corresponding test loss (1-accuracy) at best observed loss over five trials of `HomOpt` *over the base methodology for each dataset and method in the XGBoostBenchmark. Bold values indicate where* `HomOpt` *outperforms the base methodology.*

method dataset	**bayes**	**random**	**smac**	**tpe**
10101	-30.67 ± 5.42	-8.89 ± 4.16	-13.33 ± 4.16	**7.62** ± 6.67
146818	**13.33** ± 8.89	-11.43 ± 12.29	-20.00 ± 7.28	-64.00 ± 21.35
146822	-5.33 ± 3.89	-2.67 ± 4.52	-15.71 ± 6.93	**2.35** ± 6.06
168912	**1.62** ± 2.51	-10.29 ± 1.46	**8.72** ± 2.08	-3.53 ± 4.78
31	**11.67** ± 6.77	-2.50 ± 4.08	-17.14 ± 2.43	**15.71** ± 2.90
3917	-32.50 ± 2.43	-2.00 ± 5.44	-33.33 ± 2.95	-27.50 ± 8.50
53	-15.29 ± 8.44	-12.63 ± 6.14	-10.00 ± 3.24	-7.78 ± 2.83
9952	**3.51** ± 3.80	**10.82** ± 1.23	**4.56** ± 1.43	-4.29 ± 1.07